NASA-TM-109,013

NASA Technical Memorandum 109073

NASA-TM-109073 19940028612

Structural Damping Studies at Cryogenic Temperatures

Clarence P. Young, Jr.
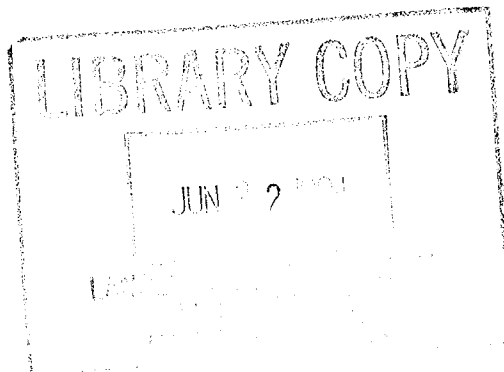*North Carolina State University, Raleigh, North Carolina*

Ralph D. Buehrle
Langley Research Center, Hampton, Virginia

May 1994

National Aeronautics and
Space Administration
Langley Research Center
Hampton, Virginia 23681-0001

TABLE OF CONTENTS

LIST OF TABLES AND FIGURES

SUMMARY

Results of an engineering study to measure changes in structural damping properties of two cryogenic wind tunnel model systems and two metallic test specimens at cryogenic temperatures are presented. Data are presented which indicate overall, a trend toward reduced structural damping at cryogenic temperatures ($-250°$F) when compared with room temperature damping properties. The study was focused on structures and materials used for model systems tested in the National Transonic Facility (NTF). The study suggests that the significant reductions in damping at extremely cold temperatures are most likely associated with changes in mechanical joint compliance damping rather than changes in material (solid) damping.

INTRODUCTION

This study was carried out in support of wind tunnel research at the National Transonic Facility located at the NASA Langley Research Center (LaRC). Evidence of significant reduction in structural damping at cryogenic temperatures was initially observed at LaRC during vibration testing of a 2-D flutter model that was successfully tested in the NASA Langley Research Center 0.3-Meter Transonic Cryogenic Tunnel (0.3 Meter TCT), see reference 1. The 2-D model was constructed from 18% Nickel 200 grade maraging steel (VASCOMAX 200) which is a preferred material for cryogenic models due to its high strength and acceptable toughness at cryogenic temperatures. Interest in potential changes in structural damping was revived during the study of NTF model support vibration problems which is documented in reference 2. The buffet test reported in reference 3 and aeroelastic studies reported in references 4 and 5, suggested that further studies of this apparent phenomena were warranted. In particular, for buffet tests in cryogenic tunnels the structural damping was assumed to be constant with temperature (ref. 3).

An engineering experiment conducted at LaRC in December, 1984 failed to support the observations reported in reference 1. This study was documented in a NASA Langley internal memorandum and was conducted to examine the damping response of a simple torsional specimen at cryogenic temperatures. The specimen used was a 36 inch long, 1/2 inch diameter shaft with a 2 inch thick disk on one end, while the other end was welded to a 1/4 inch thick 14 inch square plate. The specimen was made of 18% Ni 200 grade maraging steel (VASCOMAX 200). This limited study indicated only a very slight decrease in the structural damping ratio, ζ from approximately .023 at room temperature to .021 at $-320°$F. It is important to note that the torsion specimen was a uniform rod and did not have any mechanical joints to dissipate energy, since the shaft was welded to the disk at one end and to the base plate at the other end. The torsion specimen material and geometry was chosen to correlate with the results presented in reference 1 for the 2-D airfoil which showed a significant reduction in damping for the first torsion mode. However, the 2-D airfoil described in reference 1 was mechanically clamped on the flexure end which could have contributed some damping changes to the system. Therefore, the two are not directly comparable, since the geometry and boundary conditions are quite different.

The test results presented in reference 4 suggests that increases observed in total damping of an aluminum wing may be attributed to increases in structural damping at the lower temperature. At the same time, as reported in the reference, for a thick carbon fiber delta configuration, the data indicates a decrease in structural damping at low temperature, assuming aerodynamic damping remained constant. Such observations seem to verify that structural damping is going to vary with temperature and is likely to be material, geometry, and fabrication dependent.

Changes in structural damping at lower temperatures are of paramount importance if aeroelastically scaled models are to be tested in the NTF or other cryogenic facilities. In particular, dynamic response amplitude associated with buffeting while testing at cryogenic temperatures can be increased significantly, if structural damping is extremely low. Structural damping is of greatest

importance when operating at or near resonance or the system is being excited at its natural frequency. If the forcing frequency of the disturbance coincides with a natural frequency of the model system, passive or active damping becomes a design consideration.

The purpose of this paper is to present results of a limited engineering study which was undertaken to examine trends in structural damping at cryogenic temperatures. Data are presented for actual model systems that were tested successfully in the NTF cryogenic environment and for simple beam-type specimens tested in a controlled laboratory cryogenic environment.

TEST SETUP AND PROCEDURES

The test setup and procedures used in measuring damping from free decay response data are presented in this section.

Structural Damping Definitions

The damping data presented in this paper are given in terms of the damping factor ζ, often referred to as the damping ratio, defined as $\zeta = \frac{1}{2\pi n} \ln \frac{x_o}{x_n}$. Where x_o is the initial amplitude of the free decay response and x_n is the amplitude after n cycles have elapsed. The damping factor ζ (often given in terms of % critical) is used for systems that are assumed to have viscous damping, i.e. damping is proportional to velocity. For the case of solid damping, the damping is taken to be proportional to displacement. It can be shown (ref. 6) that the solid damping factor is given by $g = \frac{\delta}{\pi}$, where δ is the logarithmic decrement defined as $\delta = \frac{1}{n} \ln \frac{x_o}{x_n}$. Therefore the solid damping factor is given by $g = \frac{1}{n\pi} \ln \frac{x_o}{x_n}$ and is related to the damping ratio by $\zeta = \frac{g}{2}$. The data presented in reference 1 are given in terms of the structural damping factor g, which is the damping parameter normally used in the formulation of the aeroelastic response of a system, e.g. flutter equations. The data presented in reference 1 and this paper were obtained using the logarithmic decrement of the free decay response and are therefore comparable and are related by a constant.

Model Systems

Initial measurements of structural damping were made on two wind tunnel model systems that were tested in the National Transonic Facility. Measurements were made of the free decay response of a High Speed Civil Transport (HSCT) model and a commercial transport model during pre-test cryogenic cycling in the NTF cryogenic chamber. These were not thermally controlled experiments, as the reference temperature reading(s) was taken from one of three thermocouples located on the force balance which is located inside the model fuselage. Therefore, the average temperatures of the sting and other model components such as the wings were not known nor were these components necessarily at equilibrium when data were recorded. The cryogenic cycling is conducted for the purpose of force balance calibration, such that efforts are made to bring the force balance at or near equilibrium but not the entire structure. For example, the cryogenic cycle for the HSCT model from ambient to −235°F and back to −44° took about 7 hours. The cryogenic cycle for the commercial transport model was conducted in a different manner in that no effort was made to bring the balance temperatures to equilibrium. The commercial transport test was dedicated to measuring structural damping and conducted as rapidly as possible due to schedule constraints. Therefore, the structural damping values for both models systems only indicate trends with change in temperature.

HSCT Model. - The physical setup for the test is illustrated in figure 2. Three miniature quartz accelerometers were installed on the model as shown in the figure. These accelerometers were successfully used for buffet testing in the NTF at cryogenic temperatures. The accelerometer leads were routed through the opening in the cryogenic chamber floor and through the model loading

2

room ceiling. A portable Fast Fourier Transform (FFT) analyzer, along with a recorder, and a printer were located in the model loading room beneath the cryogenic chamber. The model was excited by manually placing a rubber-tipped metal rod against the lower surface of the model and striking the rod lightly with a percussion hammer. Five data samples were taken at temperature intervals of approximately 50°F.

Commercial Transport. - The physical setup for the commercial transport model was basically the same as the HSCT model shown in figure 2. The accelerometer leads (cables) were routed along the sting and through a penetration at the rear of the cryogenic chamber. This setup allowed the data acquisition and analysis equipment to be located in the model bay rather than in the model loading room. The accelerometers were the same as those used for the HSCT and were located in a pattern similar to the HSCT; i.e., two along the fuselage centerline and one at an outboard location on the wing approximately 4 inches from the wing tip.

Laboratory Test Specimens

For convenience, existing test specimens (see fig. 3) that were being used for cryogenic strain gage research were chosen for this study because of availability. The specimen's were manufactured from 18% 200 grade maraging steel (VASCOMAX 200) which is used almost exclusively for NTF cryogenic force balances and is the most used material for model and sting construction. Also, an existing test specimen support fixture (fig. 4) was used for the test. The stainless steel adapter plate shown in figure 4 was the only hardware that had to be fabricated for the tests. Since the purpose of this study was to show trends in damping properties at cryogenic temperatures, the specimen geometry and support fixture were not considered to be critical to the study. Therefore, no attempt was made to design a more representative specimen and support fixture. Unfortunately, the use of the existing hardware led to a number of problems which are discussed later. Ideally, a larger specimen more representative of a model/sting configuration should provide more quantitative results. However the restricted space within the cryogenic chamber (see fig. 5) required the use of small, simple specimens.

Test Set-up. - A photograph illustrating the overall test set-up is provided as figure 5. A schematic representation of the test set-up is given in figure 6. The test specimens were mounted in the support fixture which is bolted to the chamber floor adapter plate. The specimens vibration modes were excited by deflecting the beam tip with a probe (threaded rod) which was displaced and released by a cam-type device, therefore allowing for a free decay response.

Several methods were tried for displacing the beam. Manually exciting the beam by loading it with a metal rod gave inconsistent results. An automated method was used for the second series of tests in which a stepper motor was used to position the probe under the beam tip. The beam was loaded by displacing it with the probe and moving the probe platform with the stepper motor until the probe tip slipped off the edge. The displacement amplitude for all tests was controlled by the strain gage readout under load. Unfortunately, this second approach did not work well, and was abandoned in favor of the cam device after the stepper motor was damaged beyond repair.

The manual cam type device (see fig. 5) was designed to allow constant positioning of the loading probe. Strain levels were controlled by manually operating the jack (see fig. 5) which supports the cam loading device. The beam was loaded to approximately the same strain level (approximately 1/8 inch displacement at the tip) each time data were acquired.

Instrumentation. - Initial testing was conducted by using a miniature quartz accelerometer for measuring the free decay response with one thermocouple located near the clamped end for thermal control. Subsequently, a strain gage was installed near the clamped end of the beam to provide a baseline for controlling strain (beam deflection) and also for measuring the free decay dynamic response. Since material (solid) damping is proportional to displacement, the goal was to

3

displace the specimen (at the tip) by approximately the same value for each measurement point. The displacement was not precisely controlled since Young's modulus increases slightly at cryogenic temperatures (from about 26 million psi at ambient to approximately 28 million psi at $-250°F$).

Initial testing was carried out with a uniform specimen (see fig. 3). A modified specimen also shown in figure 3 was then fabricated with a lap joint to more closely simulate a load carrying member on a model, and to include the effect of a mechanical joint. After tests were conducted for the modified specimen, it was felt that better thermal control was needed to assure that the beam was at or near equilibrium temperature when excited. As a result, three additional thermocouples were installed on each of the specimens. The final test configurations illustrating the thermocouple installations are shown in figures 7 and 8.

In order to assure that the thermocouple strain gage wires did not affect the damping response, the wires were taped to the support frame with a large amount of slack. The accelerometer wires are small enough to be negligible. Dynamic response tests were conducted with the maximum amount of instrumentation wire attached to the specimen and compared to the original specimens (at room temperature) with the minimal amount of wire to assure that damping and frequency for the specimens were not affected by the additional thermocouples and wiring attached to the specimens.

Problems were encountered with signal dropout of the miniature accelerometers for several of the cooldown cycles. The first problem occurred at $-300°F$, while other signal dropouts occurred when the device was at about $-260°$ to $-270°F$ for a sustained period of time. All of the accelerometers recovered either during warmup or after ambient conditions were reached. Tests were conducted at a local calibration laboratory in an attempt to duplicate the accelerometer failure modes, but the devices functioned down to $-300°F$ without an apparent problem. The fact that the accelerometers used for the structural damping experiment were completely exposed to the gaseous nitrogen was the contributing factor to the problems experienced. The test set-up at the local laboratory utilized an aluminum shield which prevented exposure to the cold gas. Initial calibration tests at the laboratory encountered signal dropout problems at cold temperatures until the shield was used. For wind tunnel model applications the accelerometers are embedded in the models and have worked very well at free stream temperatures down to $-250°F$. For those cases where accelerometer signal dropout occurred, only strain gage data were used for calculating structural damping properties.

The instrumentation for the final series of tests for both the uniform and modified specimen consisted of four thermocouples; one strain gage, and one miniature cryogenic accelerometer per specimen. Dynamic response data were recorded for both the strain gage and accelerometer response.

Data Acquisition and Processing. - Data were acquired and processed by a Fast Fourier Transform (FFT) analyzer for observing and evaluating the free decay response characteristics at each measurement point in both the time and frequency domain. The time domain data were transferred to a laptop computer for storage and for computation of damping characteristics.

The Matlab software program (see ref. 7), was used to compute the damping factor using the logarithmic decrement method. First, the data were digitally filtered to isolate a single mode of vibration. For a single mode of vibration, the free vibration of an underdamped linear system with viscous damping decays exponentially where the exponent is a linear function of the damping factor, ζ. A semilog plot of the cycle of vibration versus the peak amplitude is in theory a straight line. Therefore, a least square estimate of the straight line fit for the measured data was performed. The damping factor is then calculated from the slope of the straight line fit, $\zeta = -\text{slope}/(2\pi)$, where the slope $= \ln(x_n - x_o)/n$. The region of data to be fit was selected to minimize noise and filter end effects. Also curve fits to the data were overlayed on the measured data to verify the fit accuracy.

4

DISCUSSION OF RESULTS

Results of structural damping measurements for both the model systems and the beam type laboratory specimens are presented and discussed in the following sections. Measurements were initially made for the two wind tunnel model systems in a cryogenic chamber at NTF and were followed by the more closely controlled specimen testing in cryogenic laboratory facilities located at NASA Langley.

Model Systems

Three vibration modes for the HSCT model were of interest for measuring modal damping. These modes are described in table I and include first sting bending (5 Hz), the model pitching on the balance (16 Hz), and first wing bending at approximately 50 Hz. Unfortunately, due to a significant DC signal shift in the accelerometer signals, the 5-Hz mode response data could not be analyzed with any degree of accuracy. Filtering the signal gave a clean sinusoidal response for the 16-Hz mode, while the wing mode response was a complex sinusoid containing a beat frequency due to the presence of a 54-Hz antisymmetric wing mode.

A plot of the structural damping factor, ζ, for the 16-Hz mode (model pitching on balance) as a function of temperature is given in figure 9. Note from the figure that damping is reduced from 0.012 at ambient to a minimum of 0.004 at $-150°$F. The measured damping tracks closely during the warmup cycle as well. This trend in damping compares with the data given in figure 1 for the torsion mode (g_3). A similar decrease in damping is observed during cooldown for the 51-Hz wing bending mode as shown in figure 10. A reduction in damping by almost a factor of 4 from ambient to $-235°$F is indicated. The rapid increase in damping during warmup for this mode is not understood but may be due to the thin wing warming up much faster than other model and support system components. A somewhat similar trend (although reversed with temperature) is evident in the g_1 data of figure 1.

The vibration modes of interest for the commercial transport model are described in table II and include the first sting bending (11 Hz), the model pitching on the balance (18 Hz), and the first wing bending at 55 Hz. Surprisingly, the damping response for the commercial transport model did not indicate the significant reductions in structural damping that were observed for the HSCT model. The results are provided in figures 11 through 13. In figure 11, the damping reduction (when compared to the ambient value) for the sting-bending mode is approximately 33 percent at 0°F and remains about constant down to $-216°$F. The data for the 18-Hz mode (fig. 12) show very little change in damping over the temperature range, with the differences being of the order of the error in the damping calculations. This is in sharp contrast to the damping measurement on the HSCT model for basically the same mode (fig. 9). In figure 13, the lightly damped first wing bending mode showed a slight reduction from 0.0014 to 0.0010 during the initial part of the cooldown and then tended to increase slightly with temperature reduction. The increase in damping during initial warmup is similar to that observed for the HSCT wing mode.

Although the commercial transport model did not exhibit large changes in structural damping when compared to the HSCT model, there are differences between the configurations and test procedure which may have influenced the results. First of all, the cryogenic cycle was not the same, as dwell times at discrete temperatures during cooldown were less and the cryogenic cycle (cooldown and warmup) for the commercial transport was conducted faster than the HSCT. There are significant geometric differences in that the sting for the commercial transport consists of a straight section and a swept strut (represents the vertical tail), as opposed to the HSCT model which has a straight sting. Also, the commercial transport wing and fuselage are thicker than the HSCT. The larger thermal inertia, particularly for the commercial transport wing, could have resulted in much slower cooling of the wing structure than for the thinner wing on the HSCT. It should be noted

that the heat-transfer coefficient for the 18 Nickel 200 grade maraging steel (VASCOMAX 200) is very low and that a long time is required to cool the models to near equilibrium conditions. Measurement and/or calculation errors for both tests should not be significantly different.

Although the results presented in figure 9 through 13 are not precise, the data (particularly for the HSCT model) support the findings reported in reference 1. The significance of these findings is that at cryogenic temperatures, reductions in structural damping can result in greater dynamic response, at least for some structural modes, than at ambient temperatures with all other variables being held constant. In particular, at or near a resonance condition, the dynamic response amplitude is a strong function of structural damping. In actuality, during aerodynamic testing the total model system damping is composed of structural and aerodynamic damping. System stability is strongly dependent on the amount of total damping present in the system. Unfortunately, for cryogenic wind-tunnel models mounted on sting supports, there is very little that can be done to increase structural damping, either active or passive.

Mabey (ref. 5) had limited success using a passive, tuned hydraulic damper to increase the damping of a sting bending mode (6.7 Hz) for a metallic-model system tested at the Royal Aircraft Establishment (RAE). The vibrations observed in reference 5 occurred at high angles of attack and were attributed to single-degree-of-freedom buffet. In any case, the author concludes that much higher structural damping is needed for cryogenic tunnels than for conventional tunnels because of the increased magnitude of any negative aerodynamic damping relative to structural damping. He further concludes that model dynamics at high angle of attack are likely to be more critical in cryogenic tunnels than in conventional tunnels. Experience in the NTF clearly supports this observation.

The implications of large reduction in structural damping at cryogenic temperatures extend beyond just model vibrations in the NTF. Reductions in structural damping could be a major factor contributing to NTF model support system vibrations in the yaw plane which is reported in reference 2. During the course of the reference investigation, it was felt that changes in structural damping (along with other variables) could be contributing to increased vibration levels after tunnel cold soak of 1 to 2 days, which was the major tunnel operational variable influencing yaw vibration levels. This study suggests that active or passive damping of the Arc Sector and fixed fairing motions (see ref. 2) could significantly attenuate vibrations in the yaw plane. This is particularly true if aerodynamic resonance or hump-mode flutter instabilities are developing under certain cryogenic operating conditions as predicted by the analyses reported in references 8 and 9.

The findings for the model systems supported the need to explore the apparent phenomena further under more closely controlled laboratory conditions. This led to experimenting with simple beam type specimens which is discussed in the next section.

Laboratory Test Specimens

Damping was measured for the first two bending modes of vibration for the uniform and modified beam specimens. The first mode response was well defined and dominated the response measurements. The second mode response was inconsistent between test runs (possibly due to variations in boundary/test conditions) and sometimes indiscernible from the measurement noise. Therefore, the results will be presented for the first mode free decay response only.

For a given test run, the frequency and damping estimates obtained from the accelerometer and strain gage data were consistent. Since the accelerometer had signal dropout problems during several of the cooldown cycles (as discussed in the section on "Instrumentation"), the strain gage data will be presented as the basis for the following discussions.

Initial Results. - Initial testing of the uniform beam specimen gave questionable and inconsistent damping results using the standard specimen support arrangement shown in figure 4. The first mode

damping for the uniform specimen increased as temperature decreased (see fig. 14). The result was unexpected and opposite to trends indicated by the tests on the model systems. The initial results raised questions as to the validity of the data with regard to what was being measured, i.e. damping of the specimen or damping of the support system and its changes with temperature.

The first series of tests for the uniform beam were suspended due to the failure of the stepper motor used to position and load the specimen. Subsequently a modified beam specimen was fabricated with a lap joint down the center and fastened together with 2–56 machine screws. It was felt that a lapped joint specimen would be more representative of wind tunnel model hardware and provide some measure of damping associated with mechanical joint compliance when compared with the uniform specimen. For example, leading and trailing edge surfaces (e.g., flaps) for cryogenic wind tunnel models are often attached by using simple lap joints.

Initial testing of the modified specimen gave much higher damping and lower bending mode frequencies at room temperature as expected. Initial test results for the modified beam showed trends toward decreased damping at lower temperatures but results were inconsistent and generally not repeatable (see figs. 15–17). For example the questionable results during warmups suggested better thermal control was needed to assure that the test specimen was at or near equilibrium and to eliminate potentially large thermal gradients. Also, it appeared that changing boundary conditions may be affecting the results, since the clamping bolts loosened after each cryogenic cycle. During the initial tests, the torque on the clamping bolts was not controlled and fastener retention devices were not used.

During the initial series of tests, damping as a function of displacement was measured at room temperature and the results are presented in table III. Data obtained at 1/2 and twice the nominal test displacement (approximately 1/8 inch at tip as measured by strain) showed the damping ratio to be independent of displacement, or more like viscous damping, for the range of loadings used for the tests. However, for some of the specimen test points the free decay response appeared to be more linear than exponential which suggests that material damping was present as well as viscous or coulomb damping. The maximum bending stress associated with nominal strain levels in the beam was of the order of 50–60 ksi which is about the average stress (not peaks) in a cryogenic model during testing in the NTF for the 18% Ni maraging steel material which has a yield strength of 200 ksi at room temperature. The model structural design is usually based on a safety factor of 4.

Thermal Control. - Three additional thermocouples were installed on both the uniform and modified specimens (see figs. 7 and 8) for the purpose of obtaining better thermal control along the length and through the thickness of the specimen. (Note: Subsequent testing revealed that initial test data were taken for cases where very large thermal gradients (up to 60°F) existed along the length of the beam.) With the additional thermocouples in place, the test specimen could be brought to very near equilibrium conditions before data were taken.

Boundary and Lap Joint Effects. - Once it became clear that measured values of damping and frequency at ambient temperature changed significantly with each test set-up, boundary conditions and lap joint tightness were varied to measure sensitivity of the response. Results of the sensitivity study are presented in table IV. Note from table IV that both structural damping and natural frequency are strongly dependent on boundary conditions and lap joint compliance (tightness). For example, the damping factor ζ, varies from 0.0017 (clamping bolts tight) to 0.0087 (clamping bolts finger tight), with corresponding frequency changes from 47.4 Hz (clamping bolts tight) to 42.3 Hz (clamping bolts loose). Also note the effect of loosening the 2-56 lap joint screws. For example, structural damping ζ, for the 2-56 screws tight was measured at 0.0017 and increased to 0.0063 when the screws were loosened with a corresponding reduction in frequency from 47.4 Hz (screws tight) to 46 Hz (screws loose). The sensitivity study suggested that inconsistent results observed

in the initial tests were strongly affected by changes in test specimen boundary conditions, and/or mechanical joint compliance brought about by extremely cold temperatures. It became obvious that better control over the boundary conditions and lap joint tightness would be necessary to obtain consistent and repeatable results for the specimen tests.

In an effort to more tightly control the test specimens boundary conditions, stainless steel shim blocks were added between the support fixture and clamping blocks at the outer clamping bolt holes. Also 1/4 inch Bellville washers were used to maintain the clamping bolts preload, and locktite was applied to the bolt threads. It should be noted that for earlier tests without Bellville washers and locktite, the clamping screws breakaway torques were found to be significantly lower after cryo cycling the specimen. Loosening of the clamping bolts, is believed to have contributed to the observed increase in damping at cryogenic temperatures for the initial specimen tests.

Natural Frequency Variations With Temperatures. - For all tests on both the uniform and modified beam, natural frequencies for both modes 1 and 2 increased with decrease in temperature. These results were expected since Young's modulus for the material increases with decrease in temperature. Typical results are given in figures 18 and 19. The first mode natural frequency for the uniform specimen (fig. 18) is higher than the modified beam (fig. 19) as expected. Although the frequency increases were roughly proportional to the square root of the increase in Young's modulus, the frequency was slightly different than predicted at $-250°F$. Also it is clear that changes in boundary conditions e.g., loose versus tight clamping (see table IV) could affect the natural frequency significantly. Therefore it would seem that the increases in natural frequency with decrease temperatures are attributable to both increase in Youngs modulus and change in the boundary conditions.

Final Results. - Once the boundary condition variations were controlled consistent results were obtained for both the uniform and modified test specimens. The measured first mode damping versus temperatures for the uniform and modified beams is given in figures 20 and 21 respectively. Sample free decay response plots for the modified beam specimen are provided in figures 22 and 23 for ambient and $-250°F$ test conditions. Comparison of the data in figures 20 and 21 show that the ambient damping value for the uniform beam specimen is lower than the modified beam as would be expected.

Damping factor for the modified beam varied from 0.0045 at ambient to about 0.0026 at $-250°F$ which is approximately a 42% reduction in damping. The uniform beam damping factor varied from 0.0028 at ambient to 0.0023 at $-250°F$ for a reduction of 17%. Note the initial variation from ambient for the uniform specimen appeared to increase to about 0.0035 before a significant drop in damping is observed. This behavior is not clearly understood but is likely associated with boundary effects or test procedure. Note that the final value of damping after warmup is about 0.0037 which is higher than the initial value and comparable to 0.0035 measured at $-75°F$. The increase may be due to a boundary condition change during cooldown. Spurious or unexpectedly high values of damping were observed on cooldown of other specimens at about $-75°F$, but was not observed during the warmup cycle. The phenomena suggests some sort of relaxation or transition effect in which the specimen boundary conditions may loosen then tighten again over this temperature range. Material properties brittle transition at this temperature could also play a role in this behavior if damping is primarily material or solid damping. These results suggest that the larger variation for the modified beam is most likely due to the presence of the lap joint.

CONCLUSIONS AND RECOMMENDATIONS

Results obtained from structural damping measurements of two NTF model systems and two small beam type test specimens are presented. Results indicate that for the structures tested,

structural damping can decrease significantly at cryogenic temperatures. The decrease in damping is believed to be associated with changes in compliance across mechanical joints and boundary effects (viscous or coulomb type damping) rather than changes in material (solid damping). Experience from testing simple beam specimens suggests that damping characteristics will be configuration dependent and also depend upon cooldown rates and soak time at cryogenic temperatures. Test experience indicates that disassembly and reassembly of simple mechanical/structural systems can result in different structural damping response, due to changes in structural joint compliance. To achieve repeatability, detailed procedures must be used to minimize the variability in the mechanical connections. Structural response during transient thermal states is likely to vary. Cold soaking the structure is required to bring all components to thermal equilibrium, anywhere in between (where large thermal gradients can exist) significant variability in structural damping will be possible.

It is recommended that structural damping measurements be made at ambient and cryogenic temperatures for model systems that are specifically designed for buffet or flutter testing in cryogenic wind tunnels. In the absence of measured changes in damping, a structural damping reduction of at least 50% based on ambient damping (measured or theoretical) is recommended. Natural vibration frequency changes due to temperature only, can be approximated by changes in Young's modulus with temperature.

REFERENCES

1. Cole, Stanley R.: Exploratory Test in a Cryogenic Wind Tunnel. J. Aircraft, vol. 23, no. 12, Dec. 1986, pp. 904–911.

2. Young, C. P., Jr.; Popernack, T. G., Jr.; and Gloss, B. B.: National Transonic Facility Model and Model Support Vibration Problems. AIAA-90-1416. Presented at the AIAA 16th Aerodynamic Ground Testing Conference in Seattle, WA, June 18–20, 1989.

3. Boyden, R. P.; and Johnson, W. G., Jr.: Results of Buffet Tests in a Cryogenic Wind Tunnel. NASA TM-84520, 1982.

4. Mabey, D. G.; Boyden, R. P.; and Johnson, W. G., Jr.: Further Buffeting Tests in a Cryogenic Wind Tunnel. NASA TM-107621. September 1992.

5. Mabey, D. G.; Welsh, B. L.; and Pyne, C. R.: The Reduction of Rigid Body Response of Sting Supported Models at High Angles of Incidence. RAE TR 89-012, 1989.

6. Thomson, W. T.: Mechanical Vibrations. Second Edition, Prentice-Hall, Inc., 1953.

7. The Mathworks, Inc. *386—MATLAB User's Guide*, October 15, 1990.

8. Strganac, T. W.: A Study of Aeroelastic Stability of the Model Support System of the National Transonic Facility. AIAA-88-2033, 1988.

9. Whitlow, W., Jr.; Bennett, R. M.; and Strganac, T. W.: Analysis of Vibrations of the National Transonic Facility Support System Using a 3-D Aeroelastic Code. AIAA-89-2207, 1989.

Table I. HSCT Model System Measured Modes and
Frequencies in Pitch Plane at Room Temperature

Mode Description	Frequency, Hz
Sting Bending	5
Pitch Motion (Balance)	16
Wing Bending (1st Sym.)	50

Table II. Commercial Transport Model System Measured Modes
and Frequencies in Pitch Plane at Room Temperature

Mode Description	Frequency, Hz
Sting Bending	11
Pitch Motion (Balance)	18
Wing Bending (1st Sym.)	55

Table III. Amplitude Sensitivity Check Using Modified
Beam Specimen at Ambient Temperature

Initial Strain Reading	Frequency (Hz)	Damping Factor
1115	45.8	.00336
1135	45.8	.00338
1548	45.8	.00341
1590	45.7	.00336
2057	45.8	.00341
2060	45.7	.00343
500	45.8	.00326

Table IV. Modified Beam Frequency and Damping Response
at Room Temperature with Variable Boundary
Conditions and Lapped Joint Compliance

Measurement Number	Variables	Average Damping Factor, ζ	f(Hz)
1	Clamping Bolts Torque @ 50 in-lbs (tight), 2–56 Screws Tight	.0017	47.4
2	Clamping Bolts Torque @ 25 in-lbs, 2–56 Screws Tight	.0025	47.0
3	Clamping Bolts Finger Tight, 2–56 Screws Tight	.0087	42.3
4	Clamping Bolts Torque @ 50 in-lbs, 2–56 Screws Loose	.0063	46.0
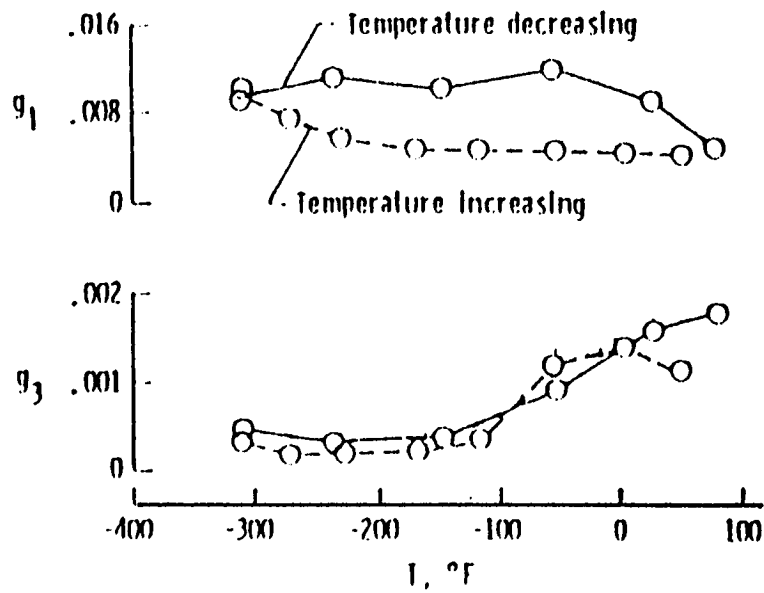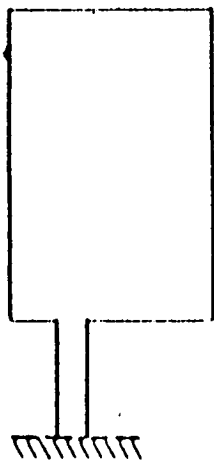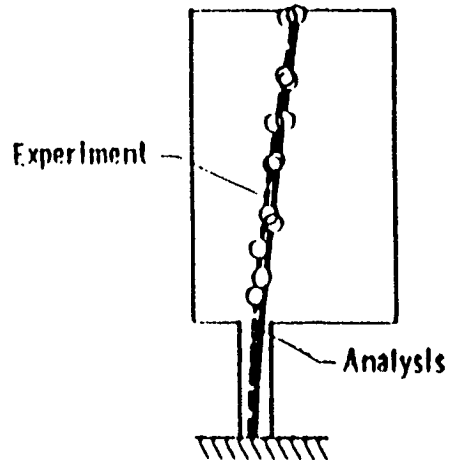
Figure 1.- Measured damping values and frequencies for flutter model tested in the 0.3-Meter Transonic Cryogenic Tunnel.

MODEL CRYO CHAMBER

STING

HSCT MODEL

RUBBER TIP

METAL ROD

■ ACCELEROMETER LOCATIONS

MODEL LOADING ROOM

ANALYZER   RECORDER

PRINTER

VIBRATION ANALYSIS
EQUIPMENT

NOTE: ACCELEROMETER WIRES
        ROUTED THROUGH OPENING
        IN CRYO CHAMBER AND MODEL
        LOADING ROOM FLOOR.

IMPULSE
HAMMER
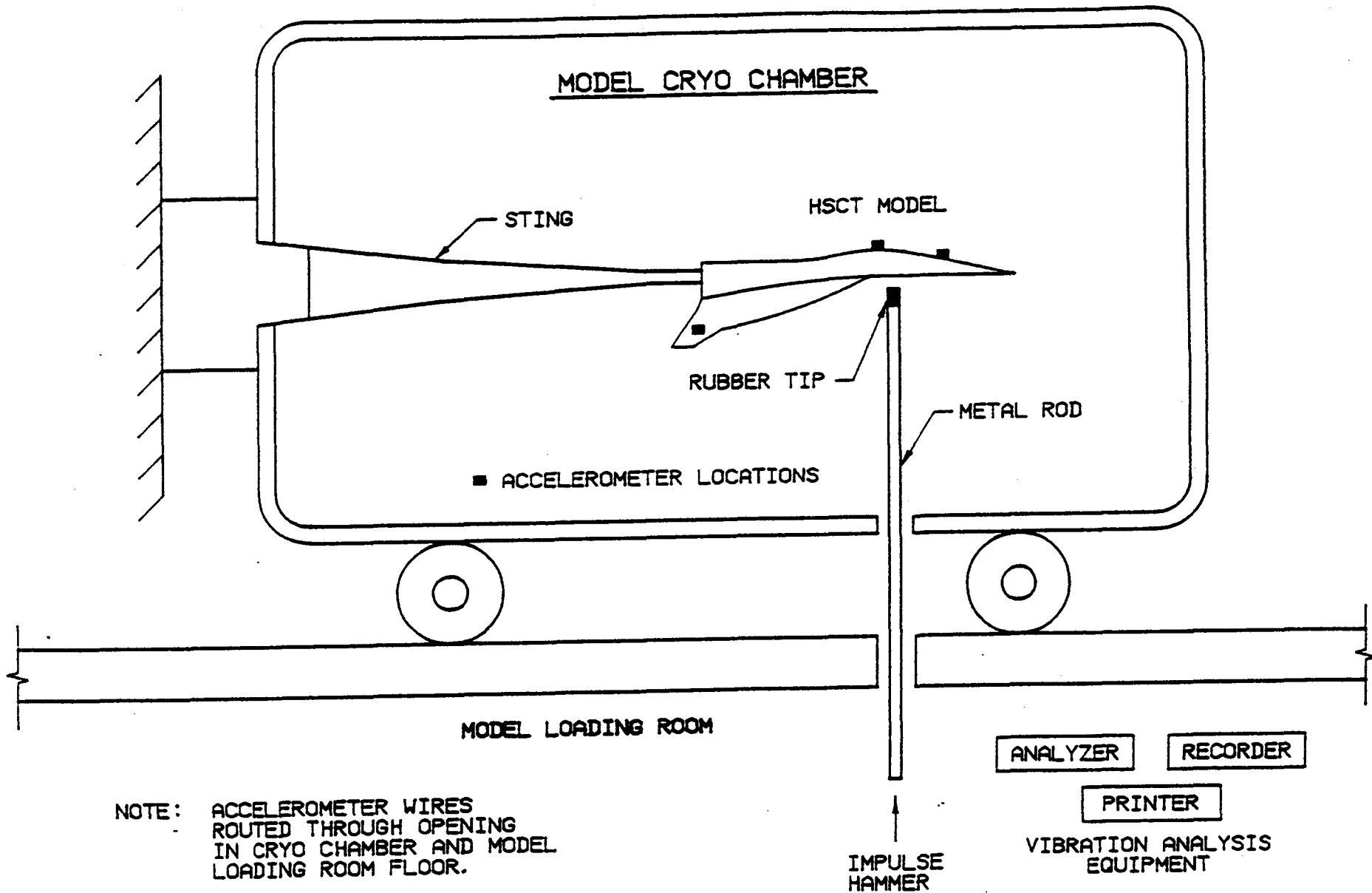
FIGURE 2.   SETUP FOR MANUALLY EXCITING THE HSCT
             MODEL SYSTEM IN THE CRYO CHAMBER

13

9/32 DIA BORE (TYP)

.25

1.00

.65

10.00

.125

1.30

UNIFORM SPECIMEN

9/32 DIA
BORE, 2
PLCS

DRILL THRU AND TAP FOR 2-56 UNC
FLAT HD CAP SCREWS (8 PLCS)

.25

1.00

.65

8 HOLES EQ. SP. @ 1' = 8.00

.44

1.30

10.00

.125

.43

.87

1.30

MODIFIED SPECIMEN WITH
LAP JOINT
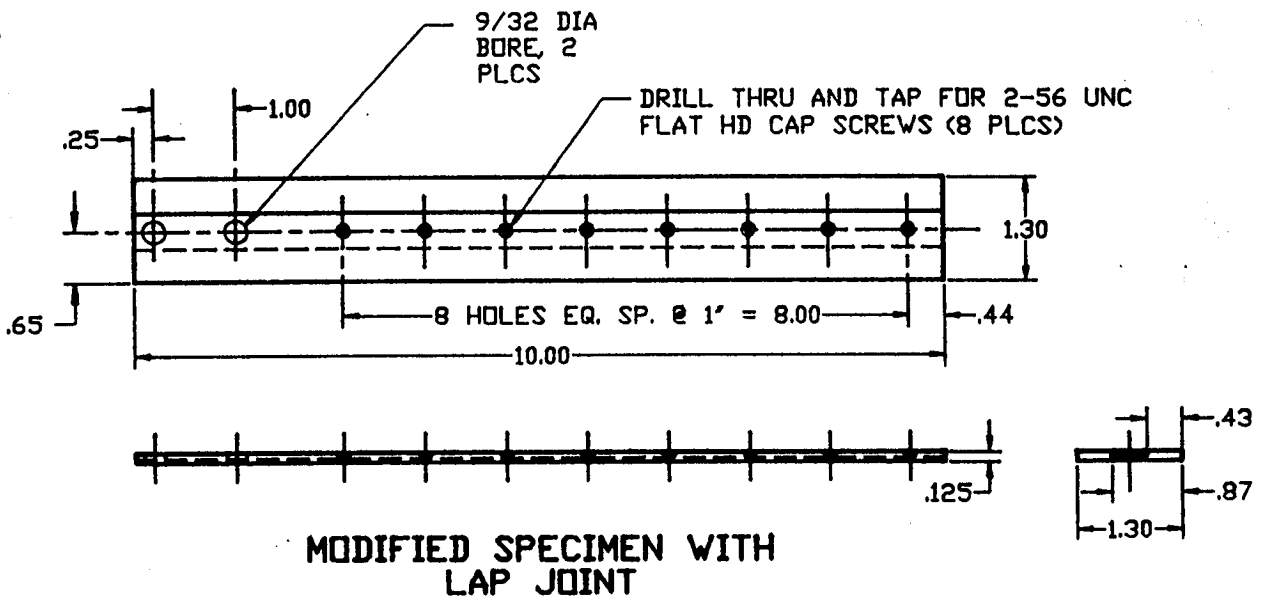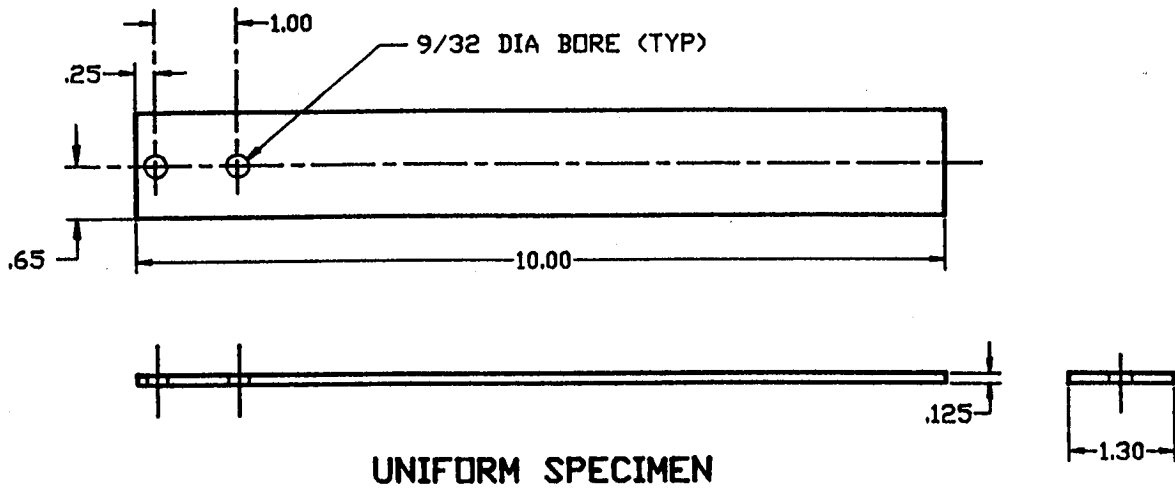
NOTE: ALL DIMENSION ARE IN INCHES

FIGURE 3   STRUCTURAL DAMPING SPECIMENS

14

Figure 4. Installation of Test Specimen on Support Fixture Inside Cryogenic Chamber

Labels in image:
- Cryogenic Chamber/Oven
- Loading Probe
- Loading Cam
- Jack
- LN₂ Dewar
- Dynamic Analyzer
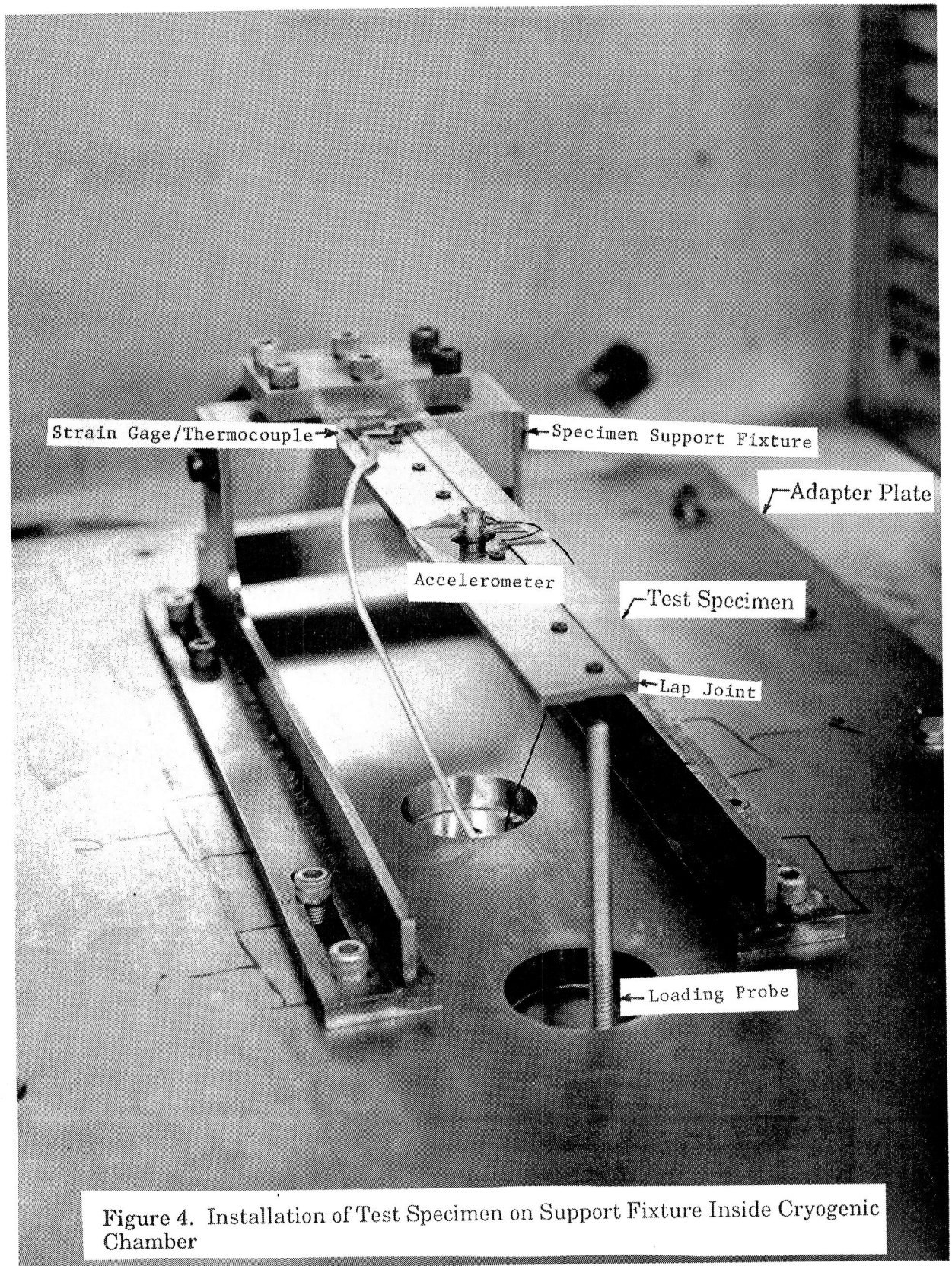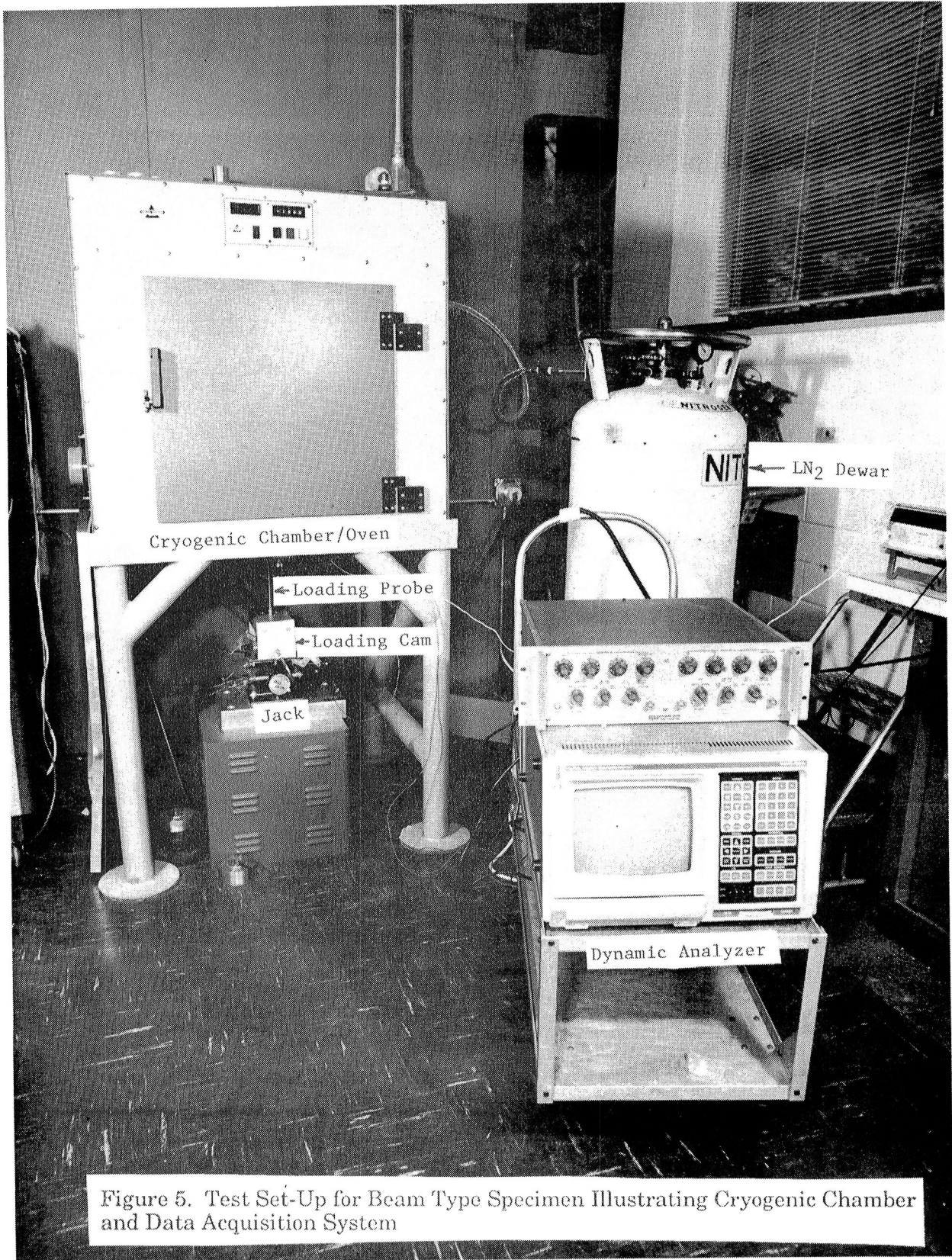
Figure 5. Test Set-Up for Beam Type Specimen Illustrating Cryogenic Chamber and Data Acquisition System
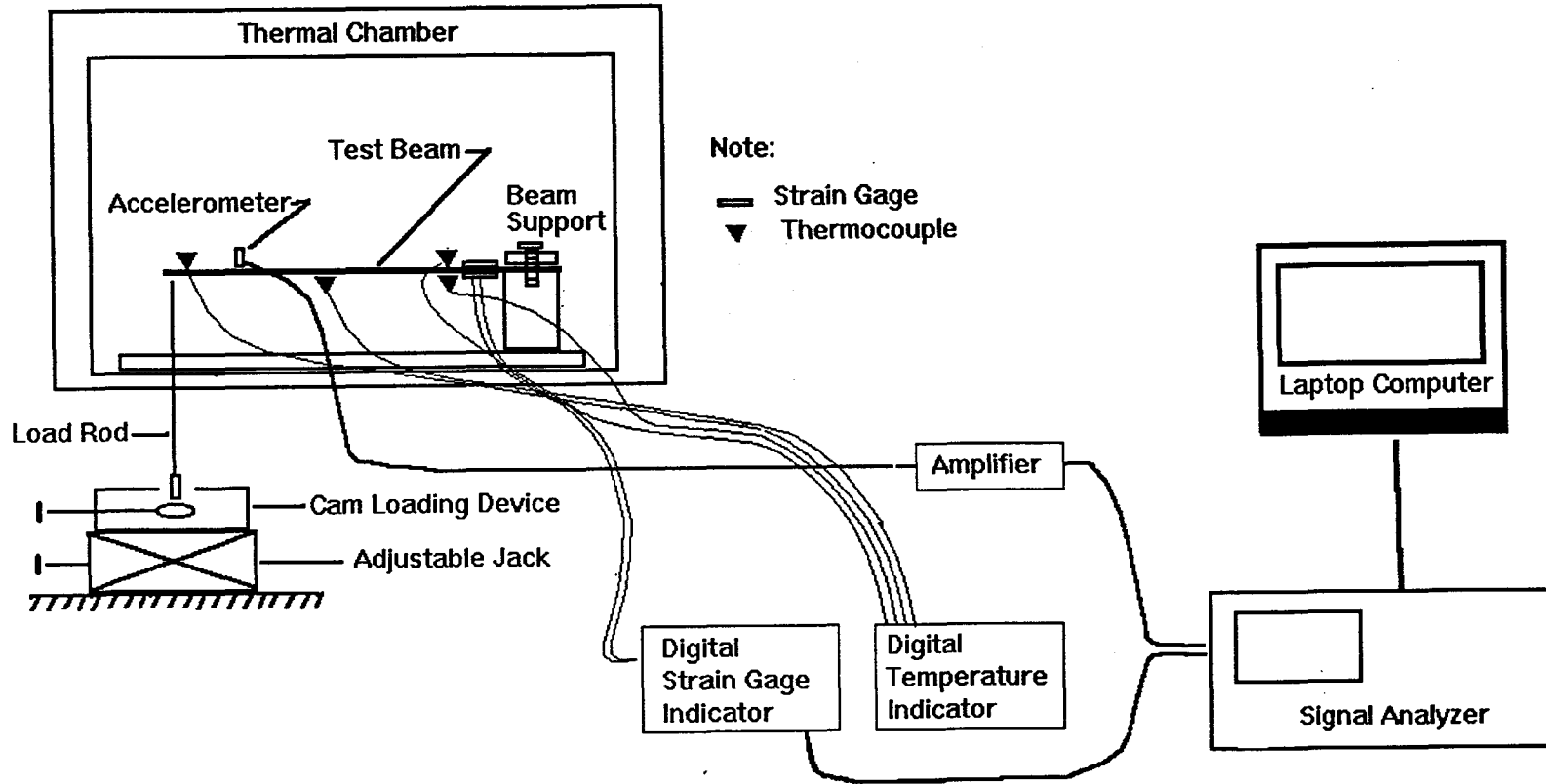
Figure 6. Schematic of Test Set-Up and Data Acquisition System

Figure 7. Uniform Beam Specimen with Strain Gages and Thermocouples Installed

Figure 8. Modified (Lap Joint) Specimen with Strain Gages and Thermocouples Installed
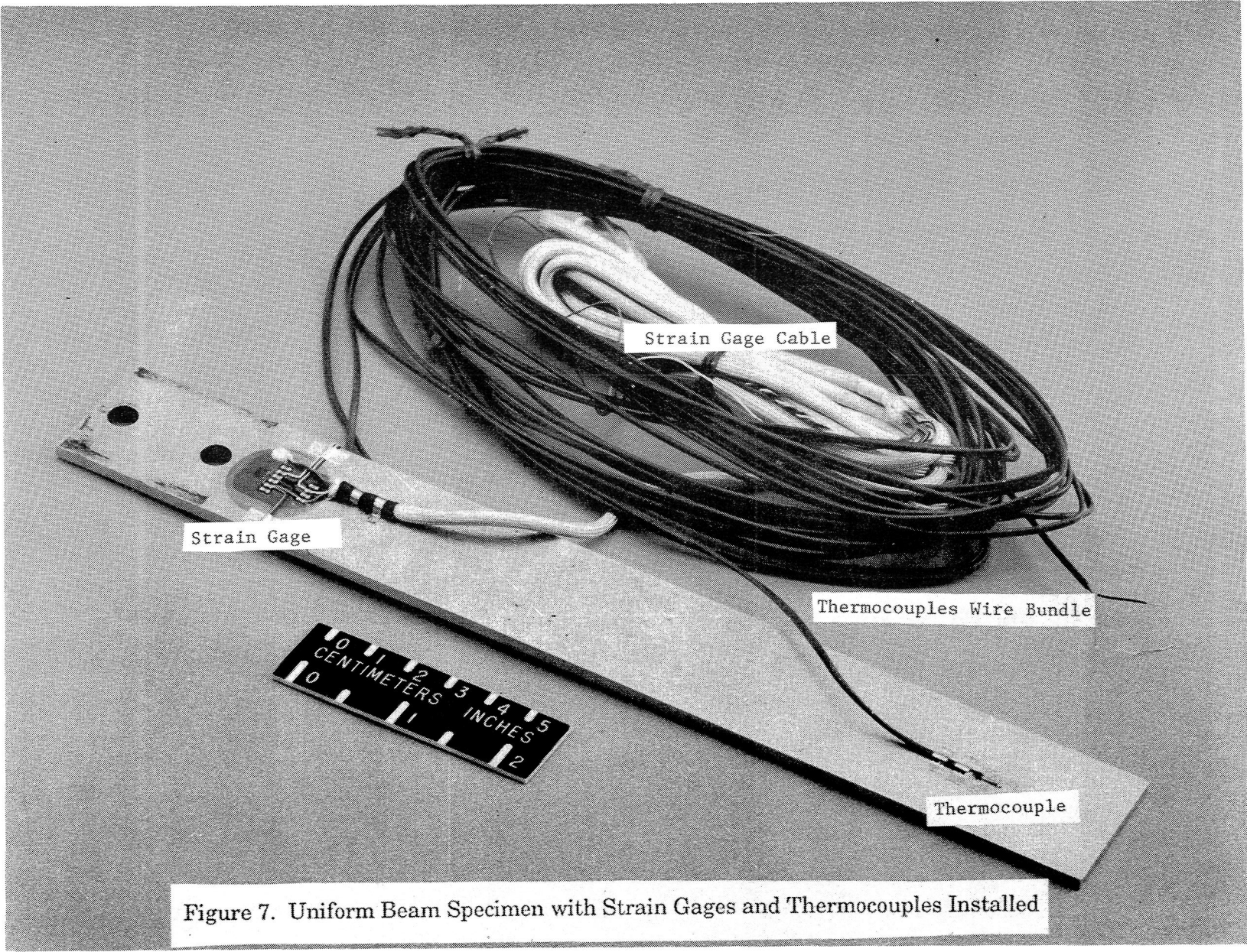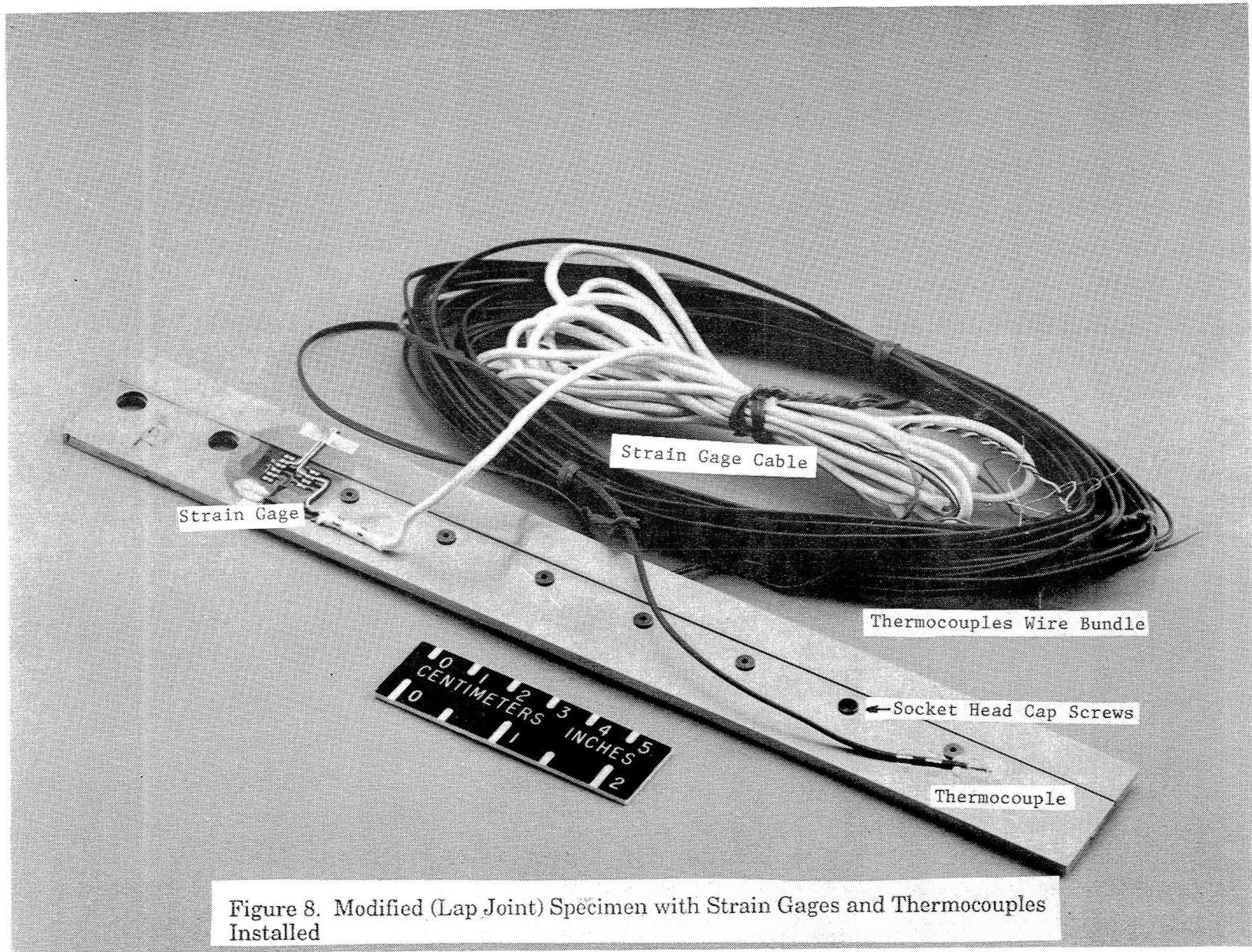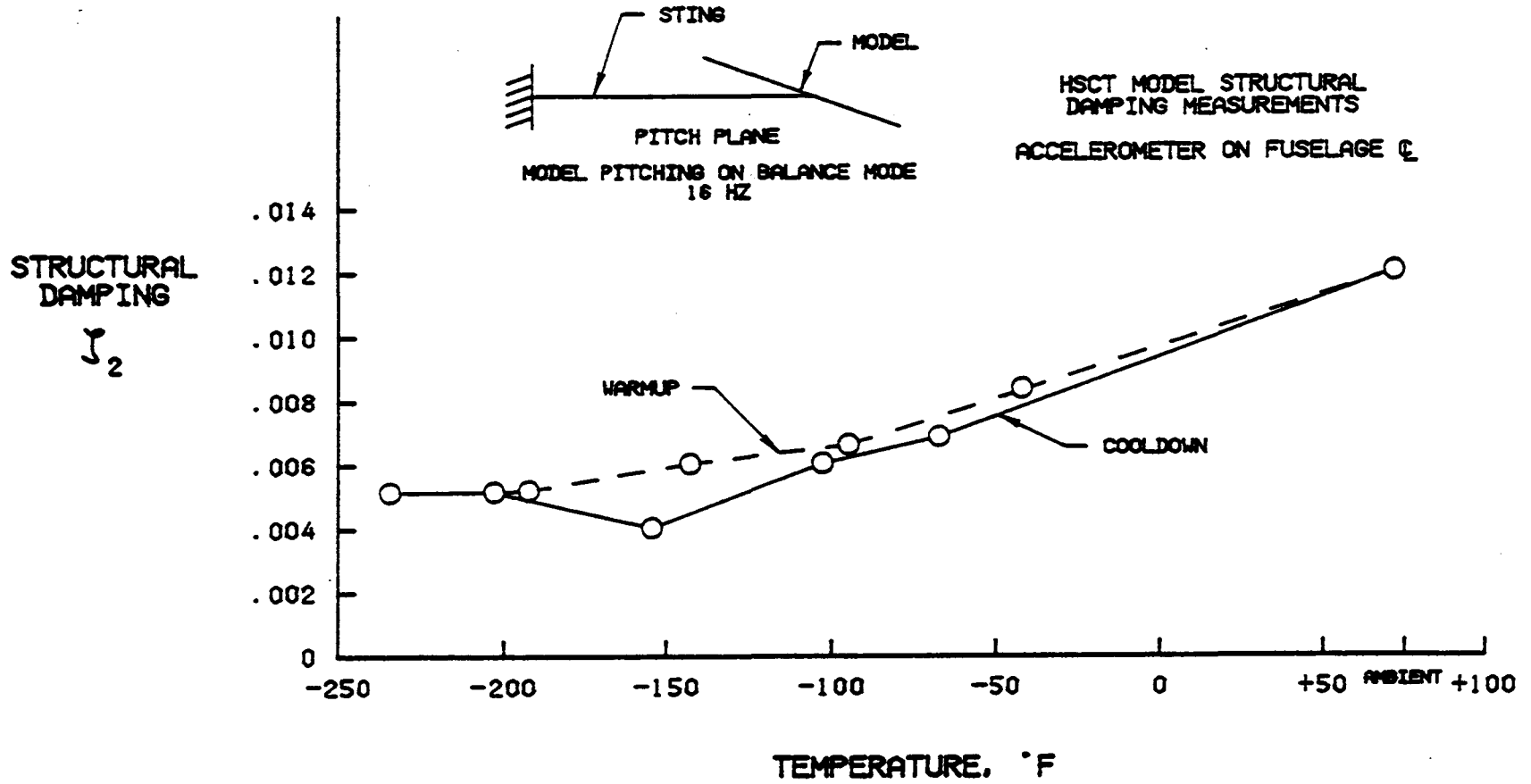
FIGURE 9 MEASURED DAMPING VALUES FOR MODE 2 - HSCT
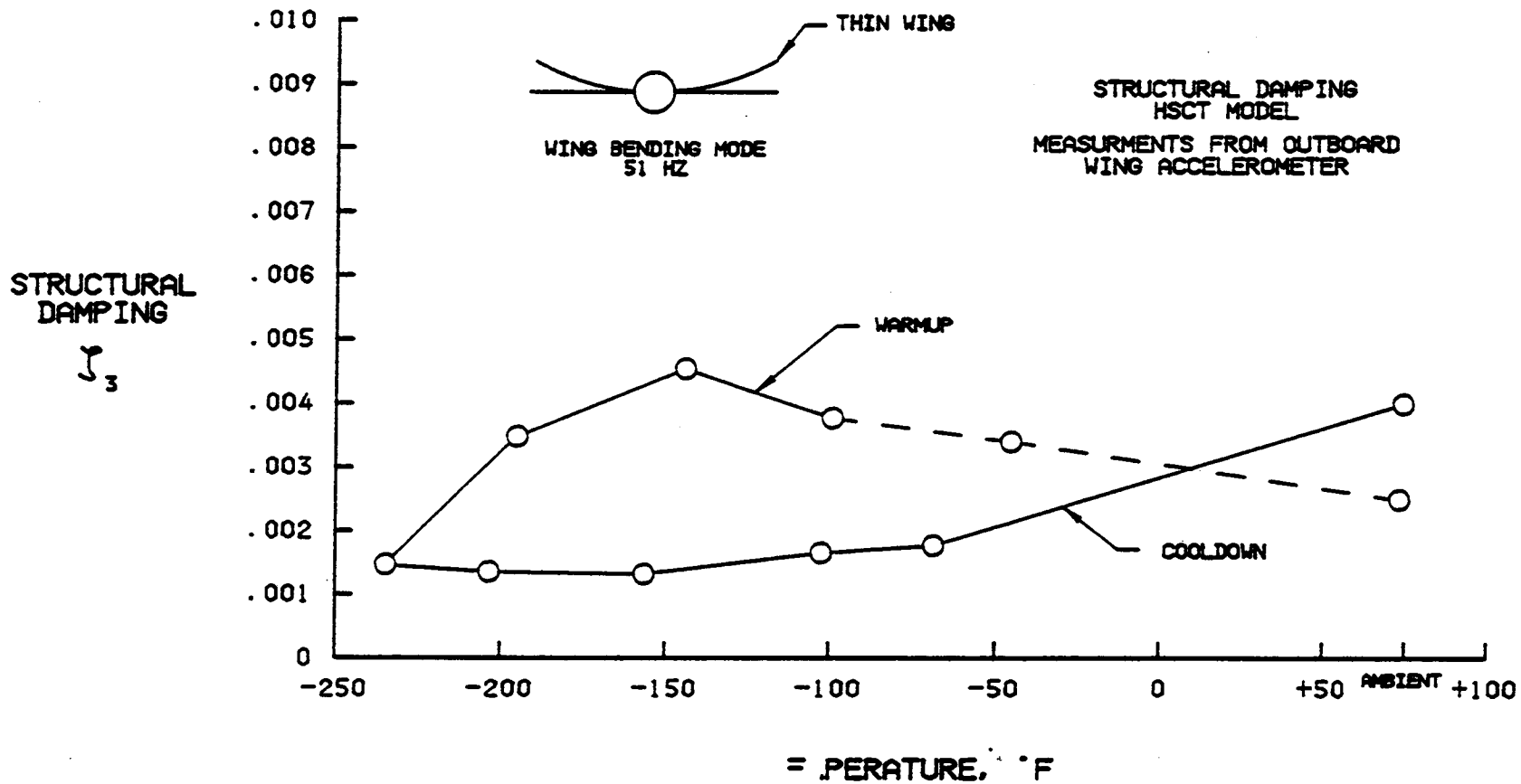
FIGURE 10 MEASURED DAMPING VALUES FOR MODE 3 - HSCT
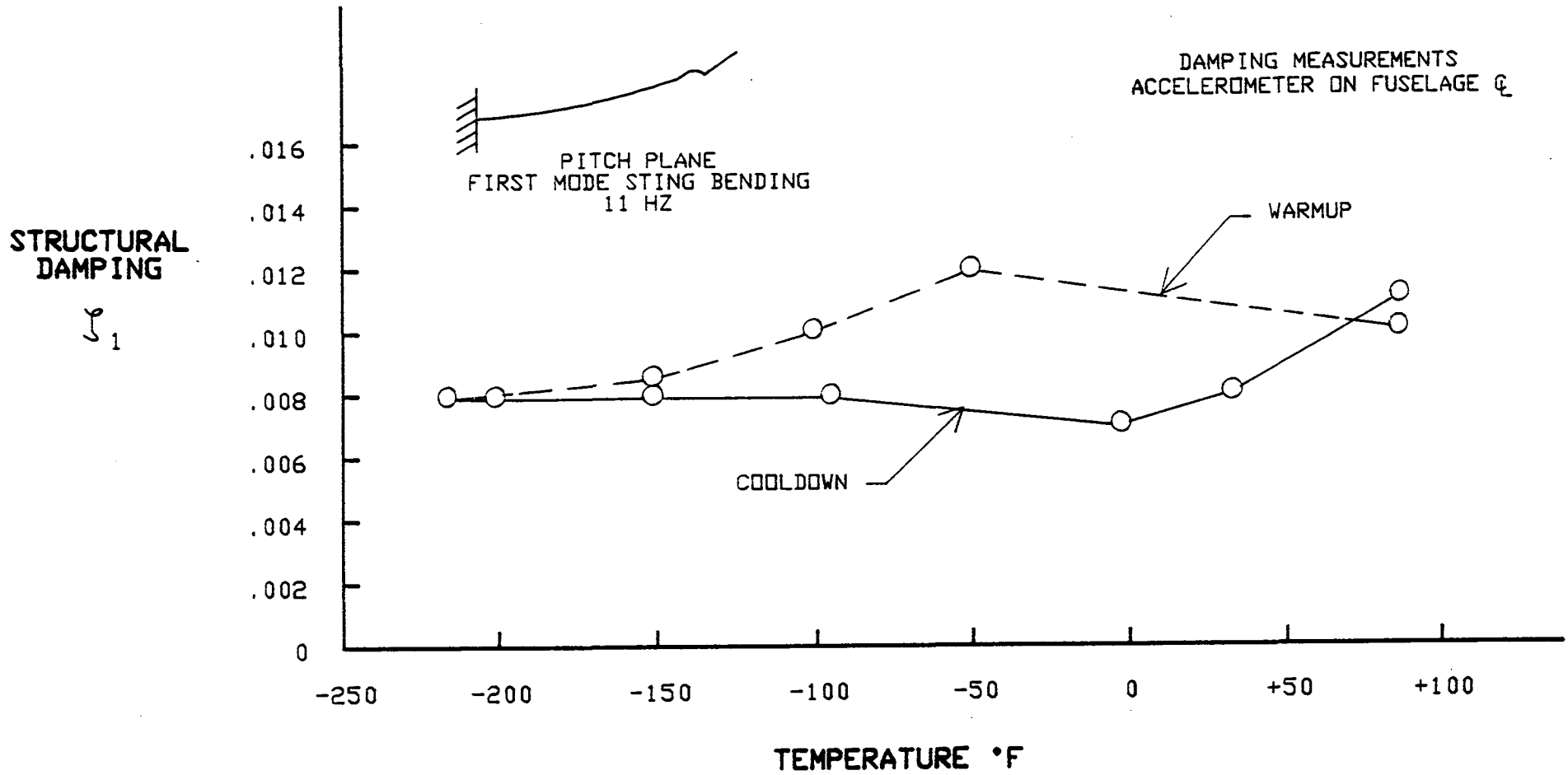
FIGURE 11. MEASURED DAMPING VALUES FOR MODE 1 - COMMERCIAL
TRANSPORT MODEL
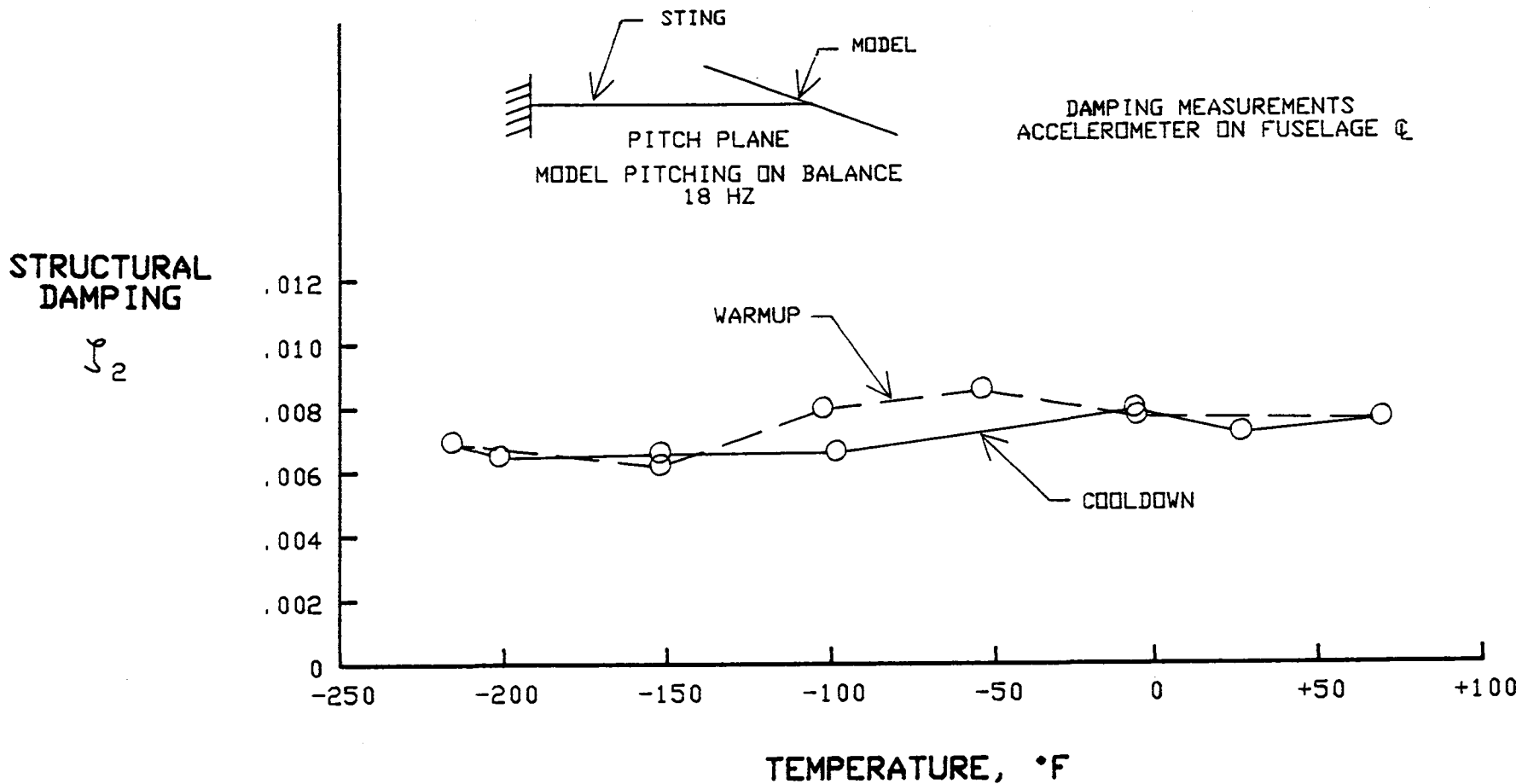
FIGURE 12. MEASURED DAMPING VALUES FOR MODE 2 - COMMERCIAL TRANSPORT MODEL
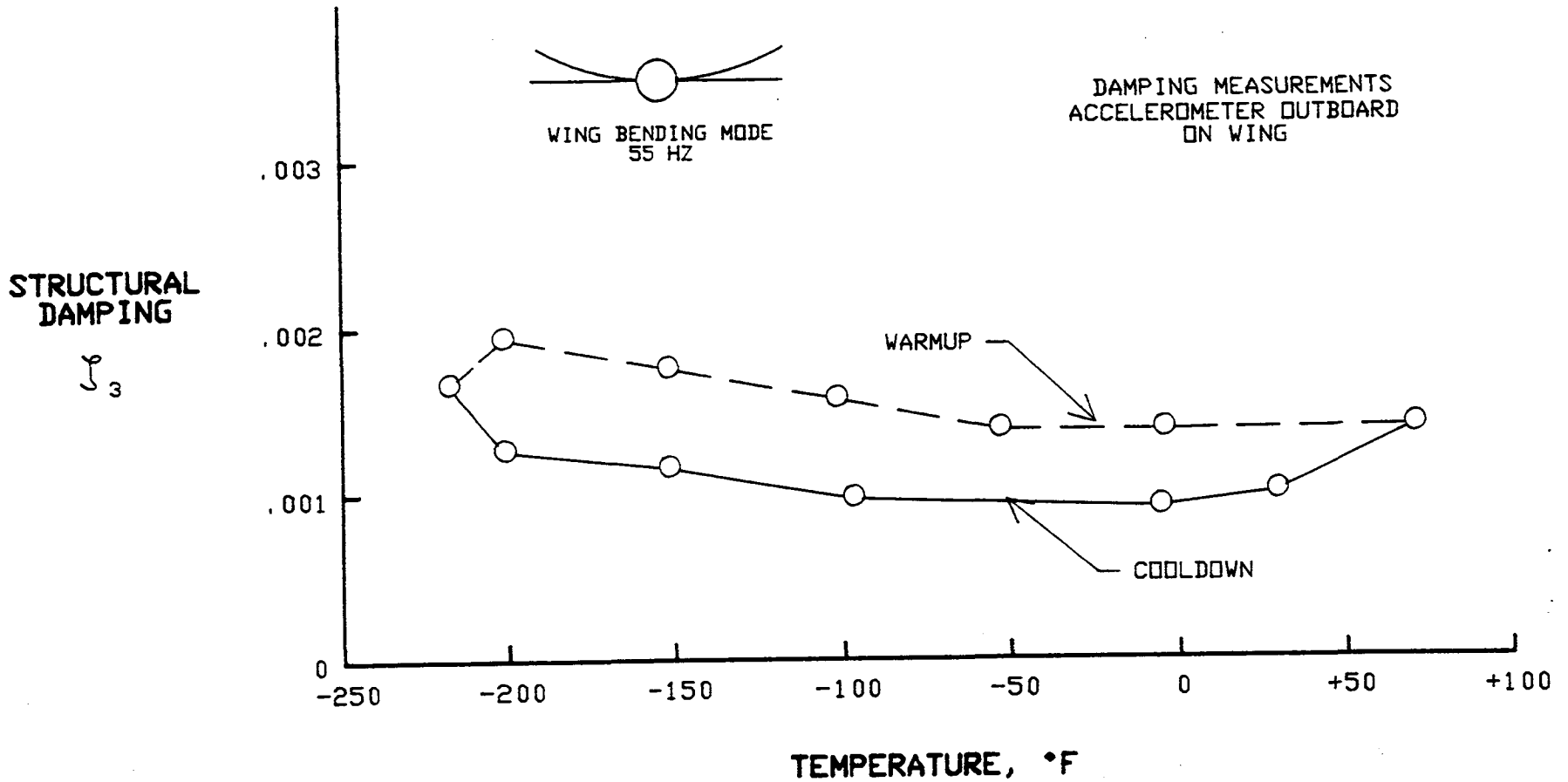
FIGURE 13. MEASURED DAMPING VALUES FOR MODE 3 - COMMERCIAL TRANSPORT MODEL
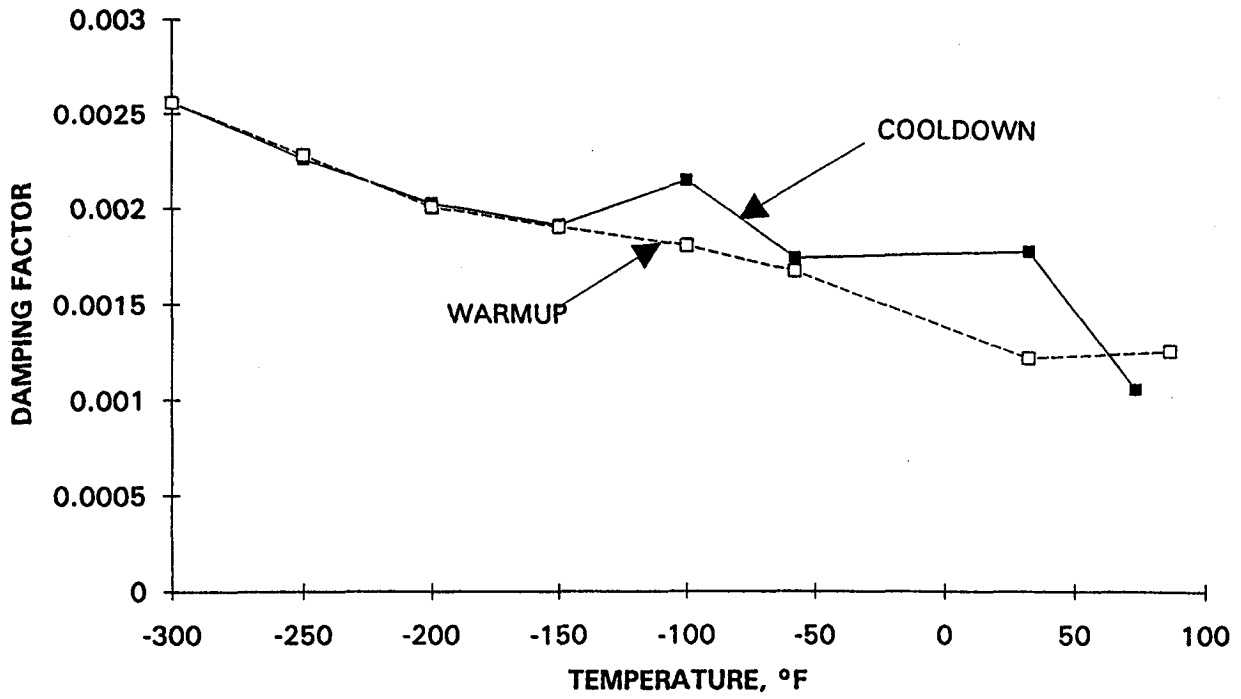
Figure 14. Damping Factor for First Bending Mode Versus Temperature for Uniform Beam Specimen From Initial Tests.
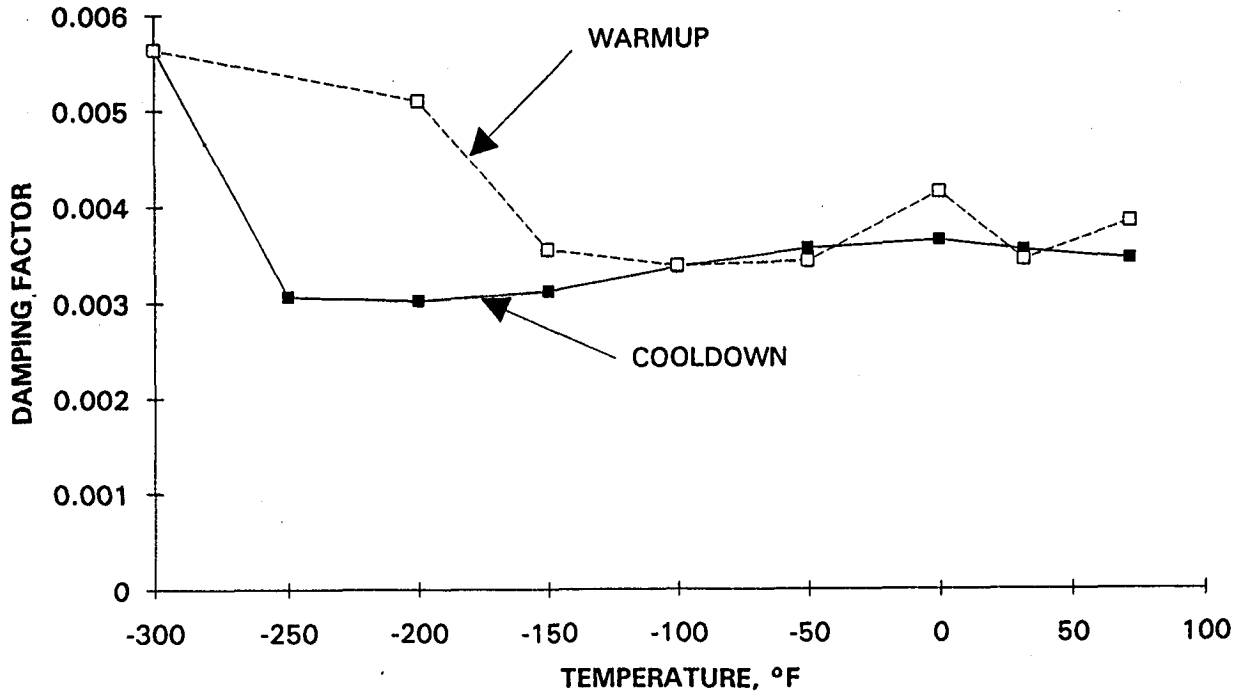
Figure 15. Damping Factor for First Bending Mode Versus Temperature for Modified Beam Specimen From Initial Tests.
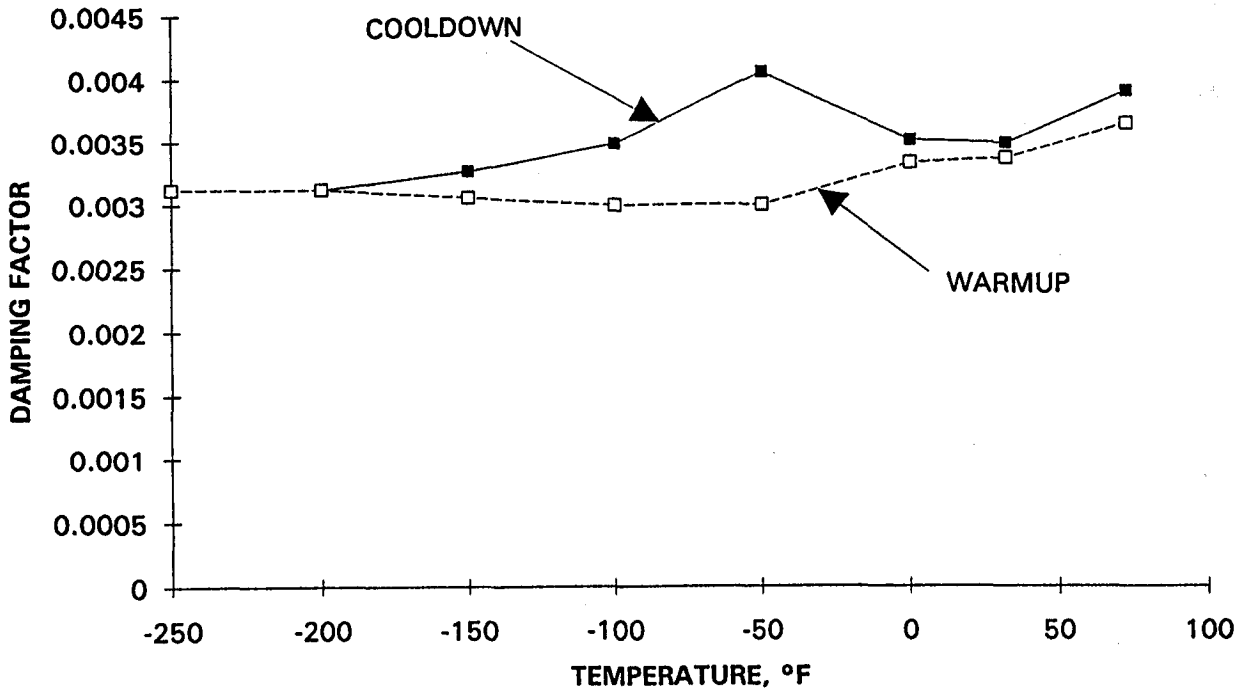
Figure 16. Damping Factor for First Bending Mode Versus Temperature for Modified Beam Specimen From Initial Tests.
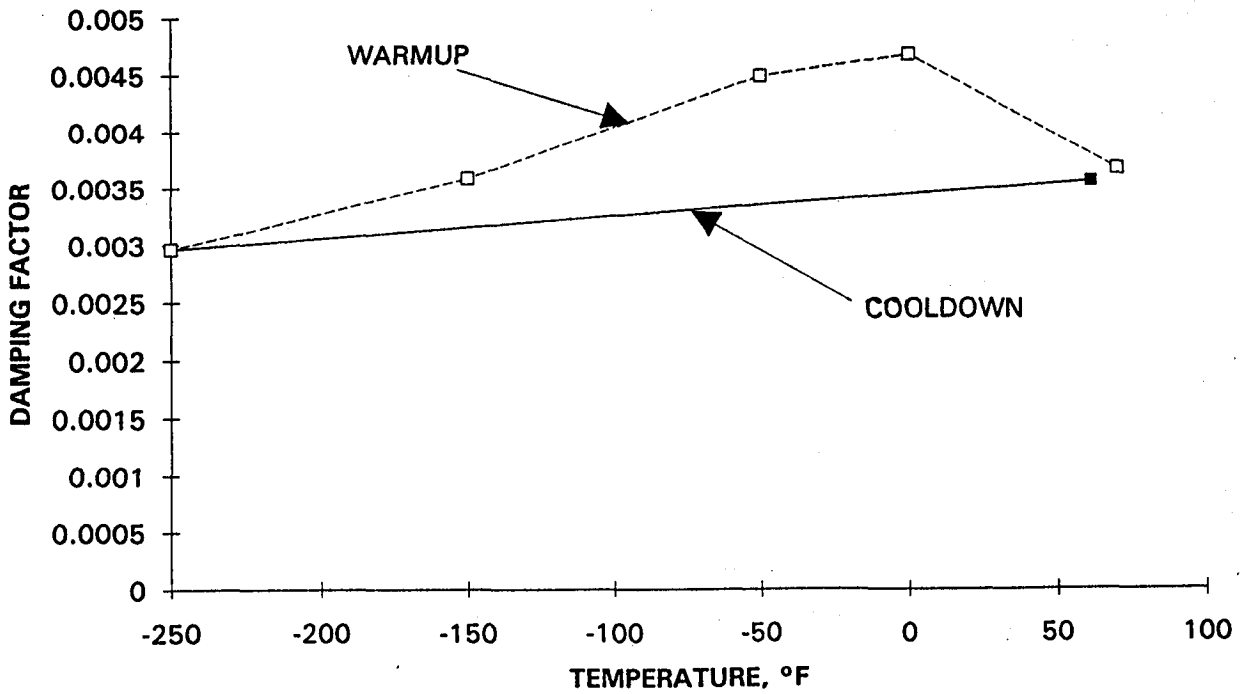
Figure 17. Damping Factor for First Bending Mode Versus Temperature for Modified Beam Specimen From Initial Tests.
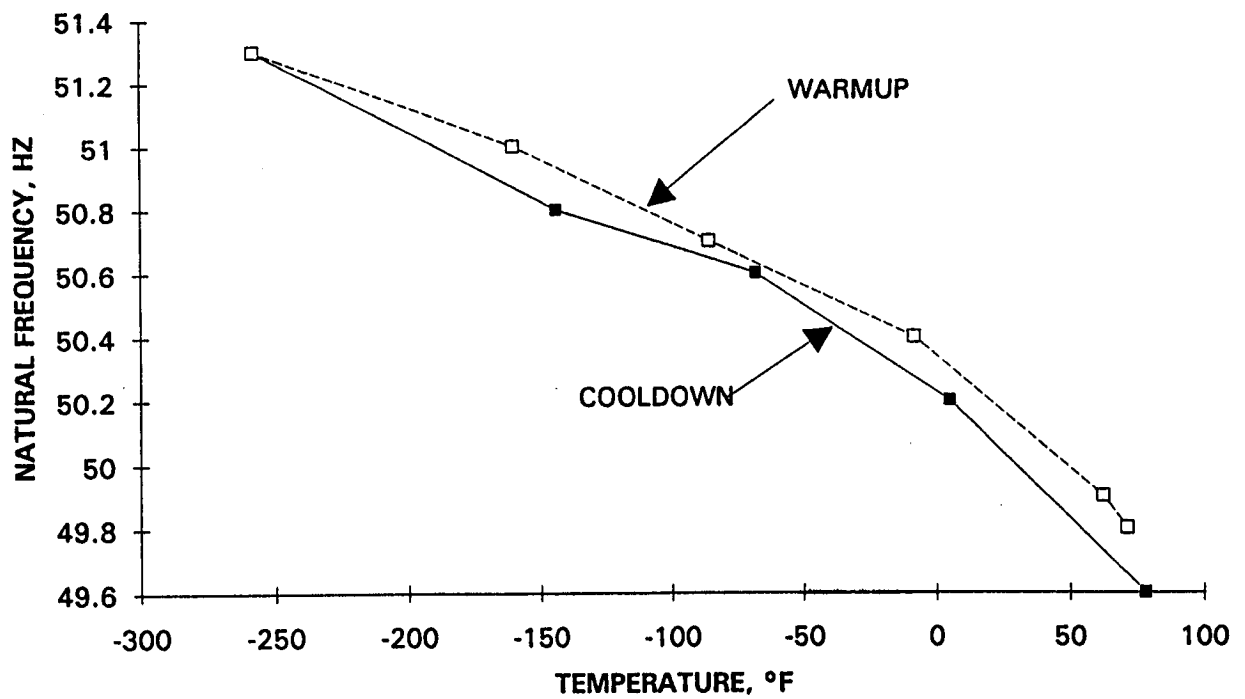
Figure 18. First Bending Mode Natural Frequency Versus Temperature for Uniform Specimen.
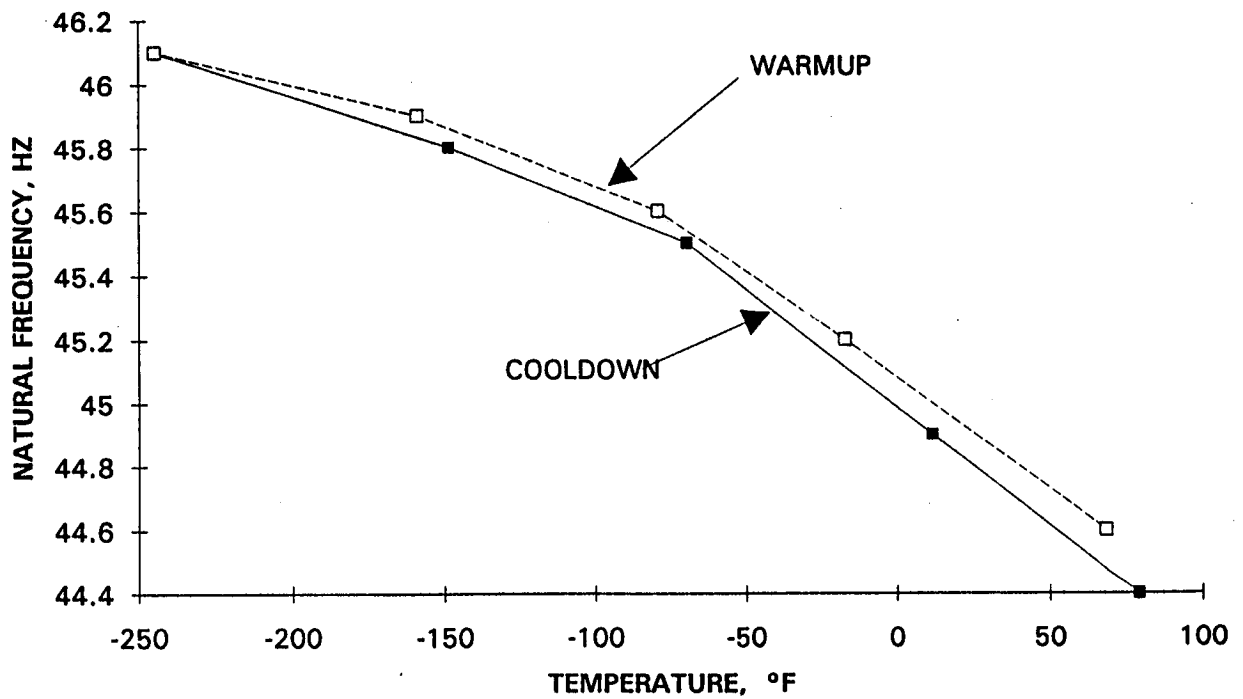
Figure 19. First Bending Mode Natural Frequency Versus Temperature for Modified Specimen.
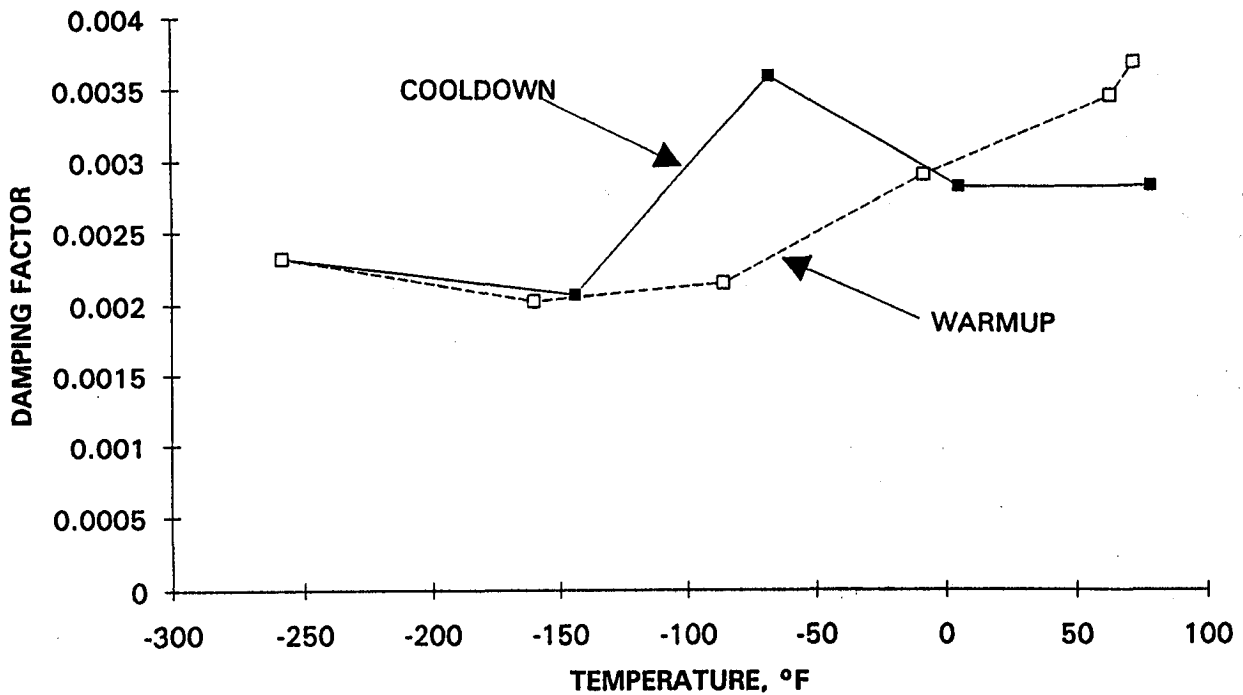
Figure 20. Damping Factor for First Bending Mode for Uniform Specimen With Thermal Control and Controlled Boundary Conditions.
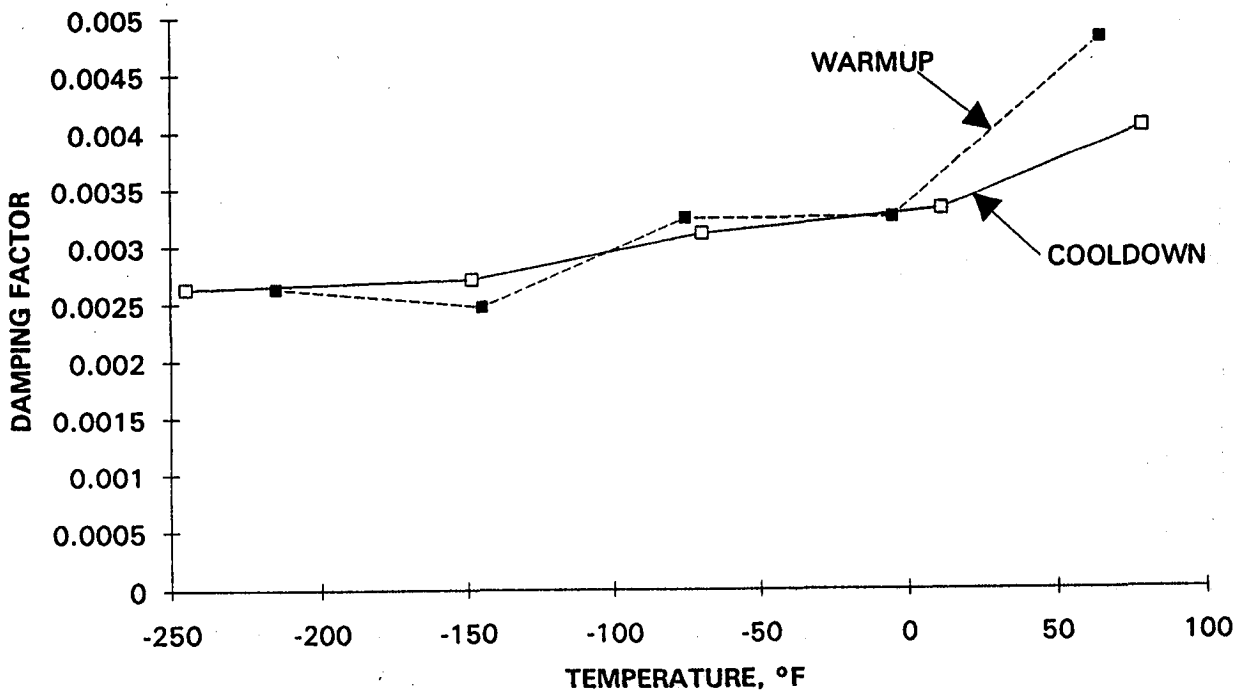
Figure 21. Damping Factor for First Bending Mode for Modified Specimen With Thermal Control and Controlled Boundary Conditions.
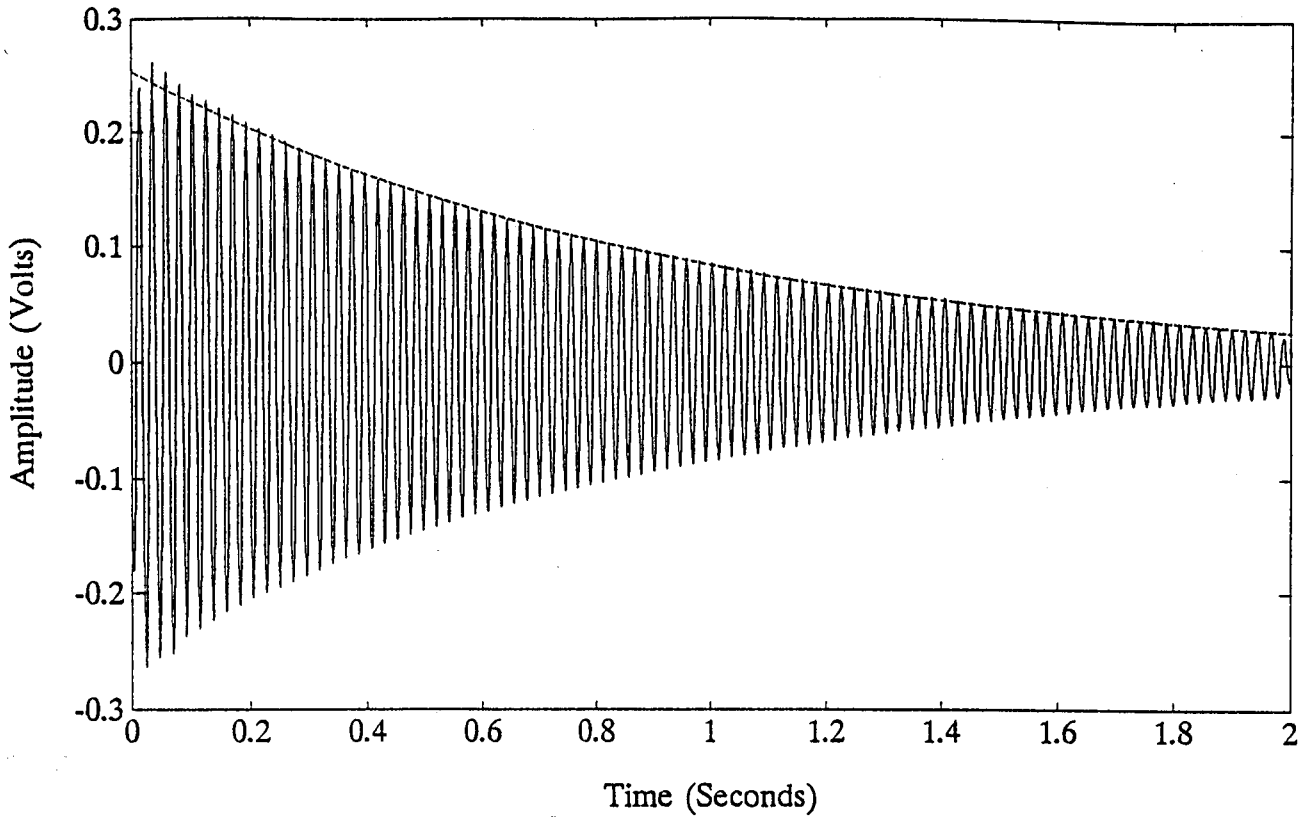
28

Frequency=44.45 Hz, Damping Factor=0.003971

Figure 22. First Bending Mode Decay Response for Modified Beam at Ambient Temperature.

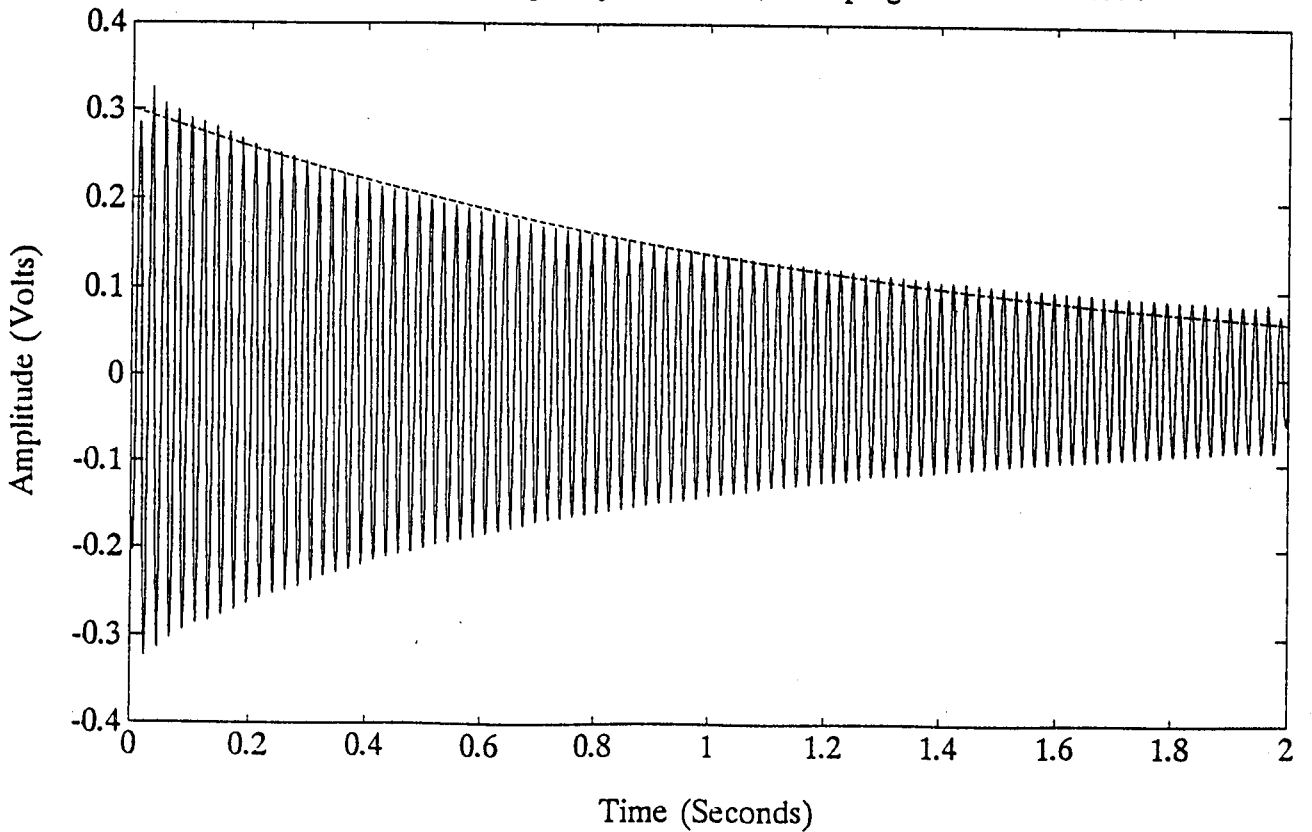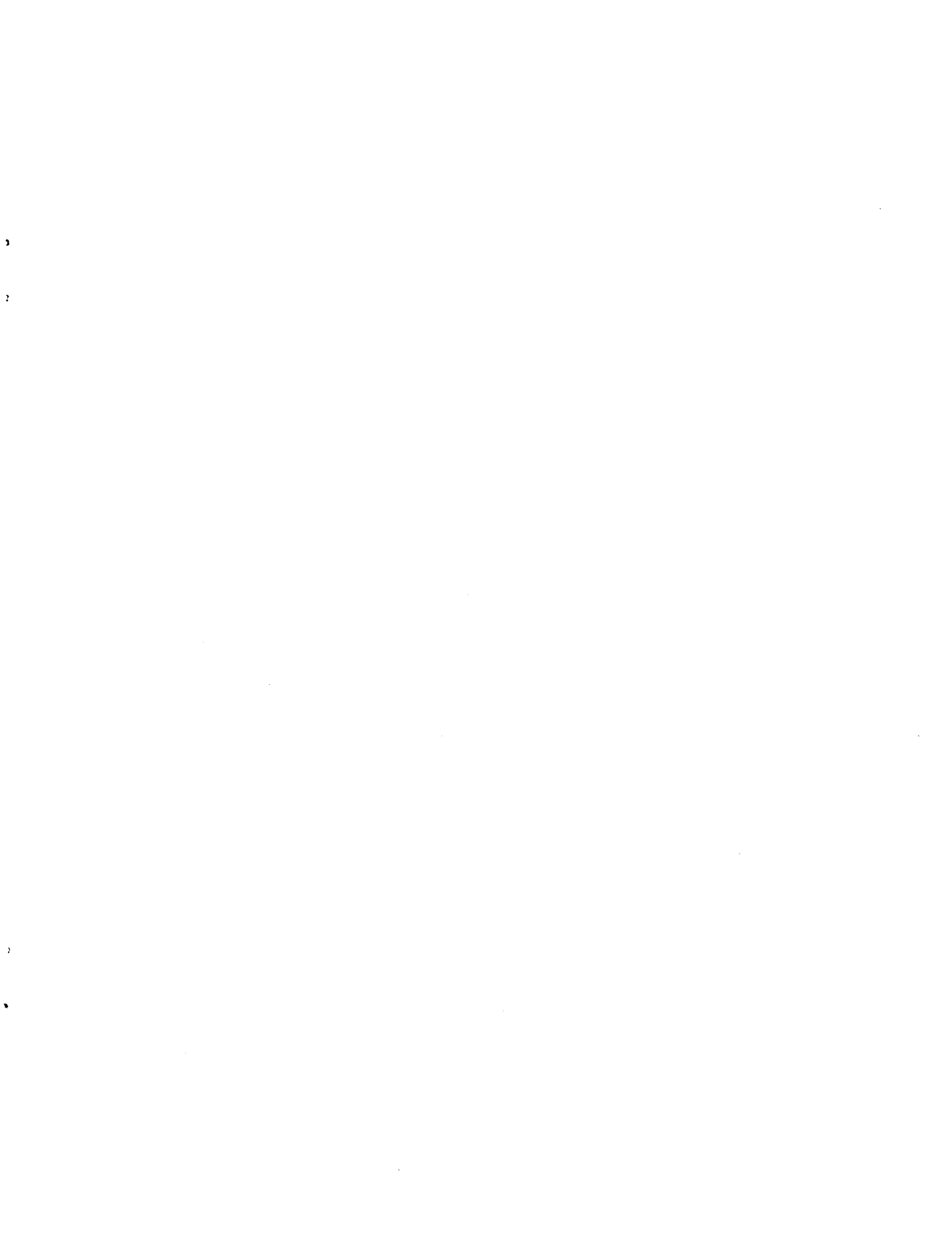Frequency=46.08 Hz, Damping Factor=0.002674

Figure 23. First Bending Mode Decay Response for Modified Beam at -250 °F.

REPORT DOCUMENTATION PAGE

Form Approved
OMB No. 0704-0188

1. AGENCY USE ONLY *(Leave blank)*	2. REPORT DATE May 1994	3. REPORT TYPE AND DATES COVERED Technical Memorandum

4. TITLE AND SUBTITLE Structural Damping Studies at Cryogenic Temperatures	5. FUNDING NUMBERS WU 505-59-54-01
6. AUTHOR(S) Clarence P. Young, Jr., and Ralph D. Buehrle	

7. PERFORMING ORGANIZATION NAME(S) AND ADDRESS(ES) National Aeronautics and Space Administration Langley Research Center Hampton, VA 23681-0001	8. PERFORMING ORGANIZATION REPORT NUMBER

9. SPONSORING / MONITORING AGENCY NAME(S) AND ADDRESS(ES) National Aeronautics and Space Administration Hampton, VA 20546-0001	10. SPONSORING / MONITORING AGENCY REPORT NUMBER NASA TM-109073

11. SUPPLEMENTARY NOTES

Young: North Carolina State University, Raleigh, NC (working at Langley Research Center, Hampton, VA)
Buehrle: Langley Research Center, Hampton, VA

12a. DISTRIBUTION / AVAILABILITY STATEMENT Unclassified - Unlimited Subject Category 39	12b. DISTRIBUTION CODE

13. ABSTRACT *(Maximum 200 words)*

Results of an engineering study to measure changes in structural damping properties of two cryogenic wind tunnel model systems and two metallic test specimens at cryogenic temperatures are presented. Data are presented which indicate overall, a trend toward reduced structural damping at cryogenic temperatures (-250°F) when compared with room temperature damping properties. The study was focused on structures and materials used for model systems tested in the National Transonic Facility (NTF). The study suggests that the significant reductions in damping at extremely cold temperatures are most likely associated with changes in mechanical joint compliance damping rather than changes in material (solid) damping.

14. SUBJECT TERMS structural damping cryogenic wind tunnel models viscous damping mechanical joint damping cryogenic testing	15. NUMBER OF PAGES 33
	16. PRICE CODE A03

17. SECURITY CLASSIFICATION OF REPORT Unclassified	18. SECURITY CLASSIFICATION OF THIS PAGE Unclassified	19. SECURITY CLASSIFICATION OF ABSTRACT	20. LIMITATION OF ABSTRACT

NSN 7540-01-280-5500

Standard Form 298 (Rev. 2-89)
Prescribed by ANSI Std. Z39-18
298-102